Sedimentary Geology 333 (2016) 15–31

Contents lists available at ScienceDirect

Sedimentary Geology

journal homepage: www.elsevier.com/locate/sedgeo

Ediacaran sedimentology and paleoecology of Newfoundland reconsidered

Gregory J. Retallack *

Department of Geological Sciences, University of Oregon, Eugene, OR 97403, USA

ARTICLE INFO

Article history:
Received 23 July 2015
Received in revised form 8 December 2015
Accepted 9 December 2015
Available online 15 December 2015

Editor: J. Knight

Keywords:
Ediacaran
Newfoundland
Paleosol
Paleoecology
Vendobiont

ABSTRACT

Ediacaran fossils of Mistaken Point and other localities in Newfoundland have been reconstructed as denizens of a deep, dark ocean, based on a turbidite interpretation of their sedimentary context. Objections to this view include geochemical indications of fresh water and volcanological and sedimentological evidence that they lived in soils of coastal plains and tidal flats. Two distinct assemblages of these fossils are recognized: a low-diversity *Aspidella–Heimalora* community on sulfidic grey paleosols (Sulfaquent) and a high diversity *Fractofusus–Charniodiscus* community on red ferruginous paleosols (Fluvent and Udept). These two assemblages and their paleosols were comparable in habitat with Phanerozoic intertidal salt marsh and coastal woodlands, respectively. Paleosol chemical composition is also evidence that Ediacaran communities of Newfoundland lived in humid, cool temperate paleoclimates, unlike arid paleoclimates of the classical Ediacaran biota of South Australia.

1. Introduction

Ediacaran fossils of Newfoundland have been considered algae, fungi, or marine invertebrates with photosymbionts in the photic zone (Fischer, 1965; Seilacher, 1984, 1989; McMenamin, 1986; Peterson et al., 2003). Other plant-like and lichen-like features of these fossils include fractal branching (Cuthill and Conway Morris, 2014), nutrient-acquiring root-like systems (Antcliffe et al., 2015), and both sexual and vegetative reproduction (Mitchell et al., 2015). An alternative view of these famous fossils of Mistaken Point and other localities in Newfoundland (Figs. 1 and 2) is that they were deep marine osmotrophic metazoans, perhaps anemones, jellyfish, or sea pens, because enclosing beds have been interpreted as turbidites (Anderson and Misra, 1968; Misra, 1971; Clapham et al., 2003; Narbonne et al., 2005; Hofmann et al., 2008; Liu et al., 2015). This study re-examines these divergent hypotheses of deep versus marginal marine habitats in two ways. First is comparative sedimentology, in which polished slabs of fossiliferous beds in the Mistaken Point Formation are compared with polished slabs and outcrops of known Phanerozoic turbidites versus intertidal–supratidal paleosols and tsunamites. Second is paleoecology, in which individual beds with fossils growing in place are evaluated as distinct kinds of communities.

Distinguishing marine from non-marine Precambrian sedimentary rocks is difficult because the biological affinities and thus habitat preferences of Ediacaran fossils remain problematic (Retallack, 2013b; Retallack, 2014b-d; Antcliffe et al., 2015; Mitchell et al., 2015). Shallow-water deposition of the Mistaken Point Formation of Newfoundland is supported by hummocky bedding, oscillation ripples, carbonate nodules, and purple-red color (Misra, 1971; Benus, 1988; Dalrymple et al., 1999). The Mistaken Point Formation also includes spindle bombs, accretionary lapilli, gas-escape structures, and ungraded crystal tuffs that could only be deposited on land, as well as trace element compositions of tuffs unique to forearc basins (Retallack, 2014a). Geochemical indices from the Mistaken Point Formation (Fig. 3), such as high (>2.8) C/S ratios (Canfield et al., 2007), are evidence of low-sulfate, freshwater paleoenvironments (Berner and Raiswell, 1984; Raiswell and Berner, 1986; Canfield et al., 2010). Furthermore low ratios (<0.2: Canfield et al., 2007) of highly reactive iron (Fe_{HR}, mainly pyrite or hematite iron) over total iron (including iron still within silicates, Fe_{TOT}) are more like soils than modern marine or lacustrine sediments (Ku et al., 2008). It could be that Ediacaran oceans and soils were totally unlike modern (Canfield et al., 2007, 2010), but scatter of these indices between freshwater and marine within the Mistaken Point Formation (Fig. 3) more likely reflects facies changes than repeated whole ocean freshenings (Retallack, 2013a). Finally, rates of sediment accumulation for the Mistaken Point Formation (0.16 ± 0.08 mm a^{-1}) were much higher than observed in distal turbidite fans (0.012–0.026 mm a^{-1}) or the deep ocean (0.002–0.009 mm a^{-1}; Retallack, 2014a). To these general indications, this contribution adds bed-scale sedimentological interpretations of the Mistaken Point Formation, and their relevance for understanding the paleoecology of fossils which grew in these beds.

* Tel.: +1 541 346 4558.
E-mail address: gregr@uoregon.edu.

http://dx.doi.org/10.1016/j.sedgeo.2015.12.001
0037-0738/

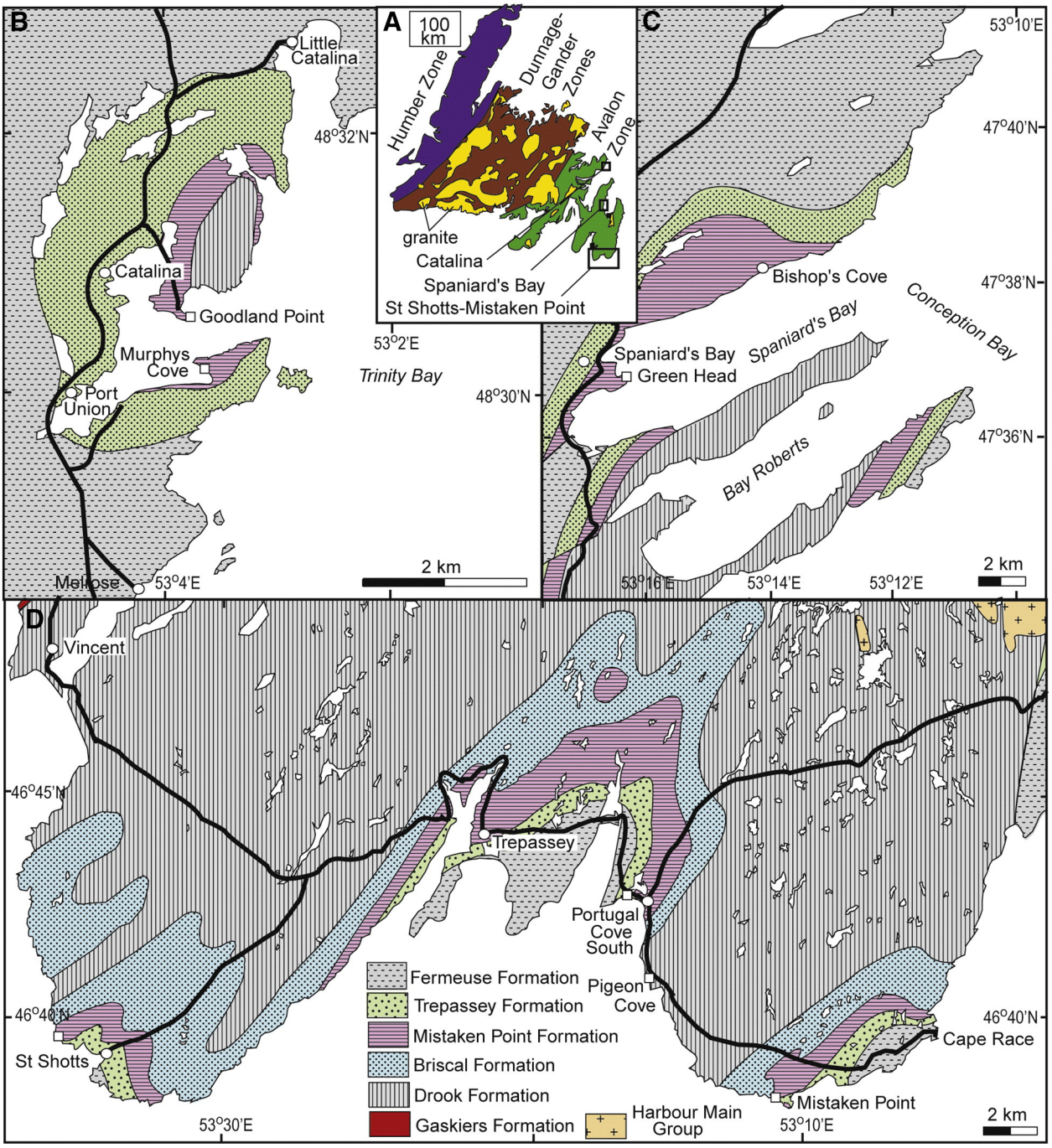

Fig. 1. Geological maps of study sites in the Avalon Peninsula of Newfoundland; A, overview of Newfoundland; B, Catalina area, eastern Bonavista Peninsula (Hofmann et al., 2008); C, Spaniards Bay, northwest Avalon Peninsula; D, Trepassey area, southern Avalon Peninsula (King, 1988).

2. Geological background

The Conception Group of the Avalon Zone of Newfoundland (Fig. 1) is well known for a variety of Ediacaran fossils, but they are most diverse in the Mistaken Point Formation (Fig. 2). Four high-precision radiometric dates within the Conception Group provide an age model for the whole sequence, with the Mistaken Point Formation dated at 565 Ma (van Kranendonk et al., 2008; Noble et al., 2015). All examined localities were within the forearc basin of the Trinity Synclinorium on granitic crust, between the Holyrood Granite (Fig. 2) exposed in the Holyrood Horst to the east and the ancient continental calcalkaline volcanic arc exposed to the west (Retallack, 2014a).

Cambrian (ca. 525 Ma) deformation metamorphosed the Conception Group to prehnite-pumpellyite facies (Papezik, 1974). Paleomagnetic directions of hematite and magnetite in the Conception Group were reset by metamorphism (Evans and Raub, 2011), but paleomagnetic directions of Marystown and Musgravetown Volcanics nearby were less severely affected and are evidence of peri-Gondwanan midlatitude locations: S34.6 ± 8.0°, S23.6 ± 8.3°, S19.1 ± 11.1°, and S24.5 ± 11.9° successively between 570 and 550 Ma (Pisarevsky et al., 2012; Thompson et al., 2012).

3. Materials and methods

To determine the sedimentological context of Ediacaran fossils in Newfoundland, this project studied the four most productive fossil

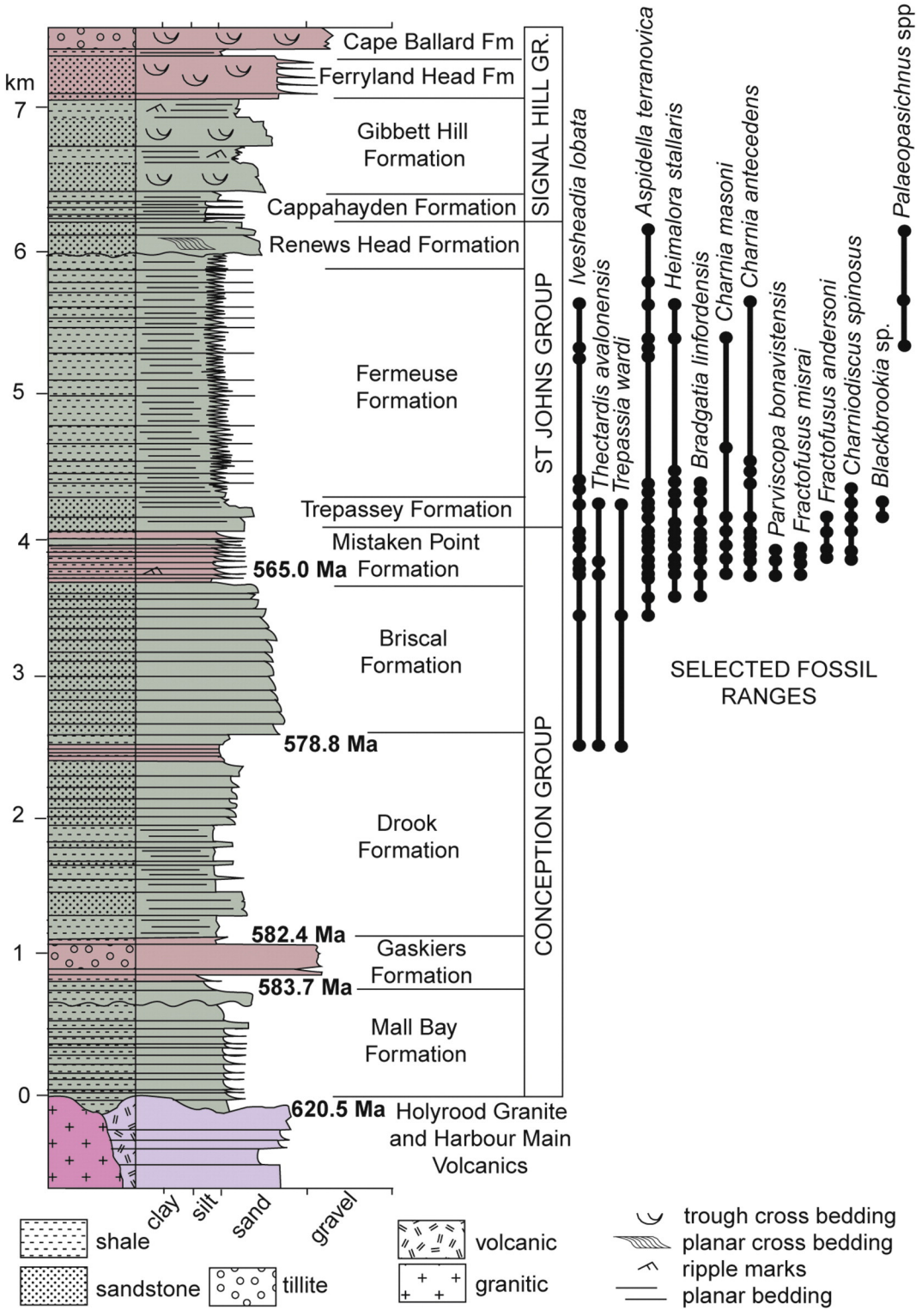

Fig. 2. Ediacaran geological succession Newfoundland with ranges of selected fossils (Clapham et al., 2003; Narbonnne et al., 2005; Hofmann et al., 2008).

localities in the Mistaken Point Formation (Benus, 1988; King, 1988; Narbonne et al., 2005, 2009): (1) Mistaken Point (Fig. 3), (2) St Shotts (Fig. 4B); (3) Murphy's Cove near Catalina (Fig. 4A), and (4) Green Head near Spaniards Bay (Fig. 4C). Other measured sections were made of the fossiliferous Drook Formation at Pigeon Cove, Briscal Formation in Bristy Cove, and Trepassey Formation west of Portugal Cove South (Fig. 5). Geographic coordinates of these localities are available on request: all are protected from unauthorized fossil collection by Newfoundland and Labrador regulation 67/11 of the Historic Resources Act (O.C. 2011–198).

This study distinguishes paleosols, tsunamites, tempestites, and turbidites by comprehensive characterization of individual beds. Petrographic thin sections from oriented rock specimens were point counted for grain size fractions and mineral content with error (Murphy, 1983) of ±2%. Specimens were also analyzed for major elements by x-ray fluorescence, for organic carbon using a Leco combustion infrared analyzer,

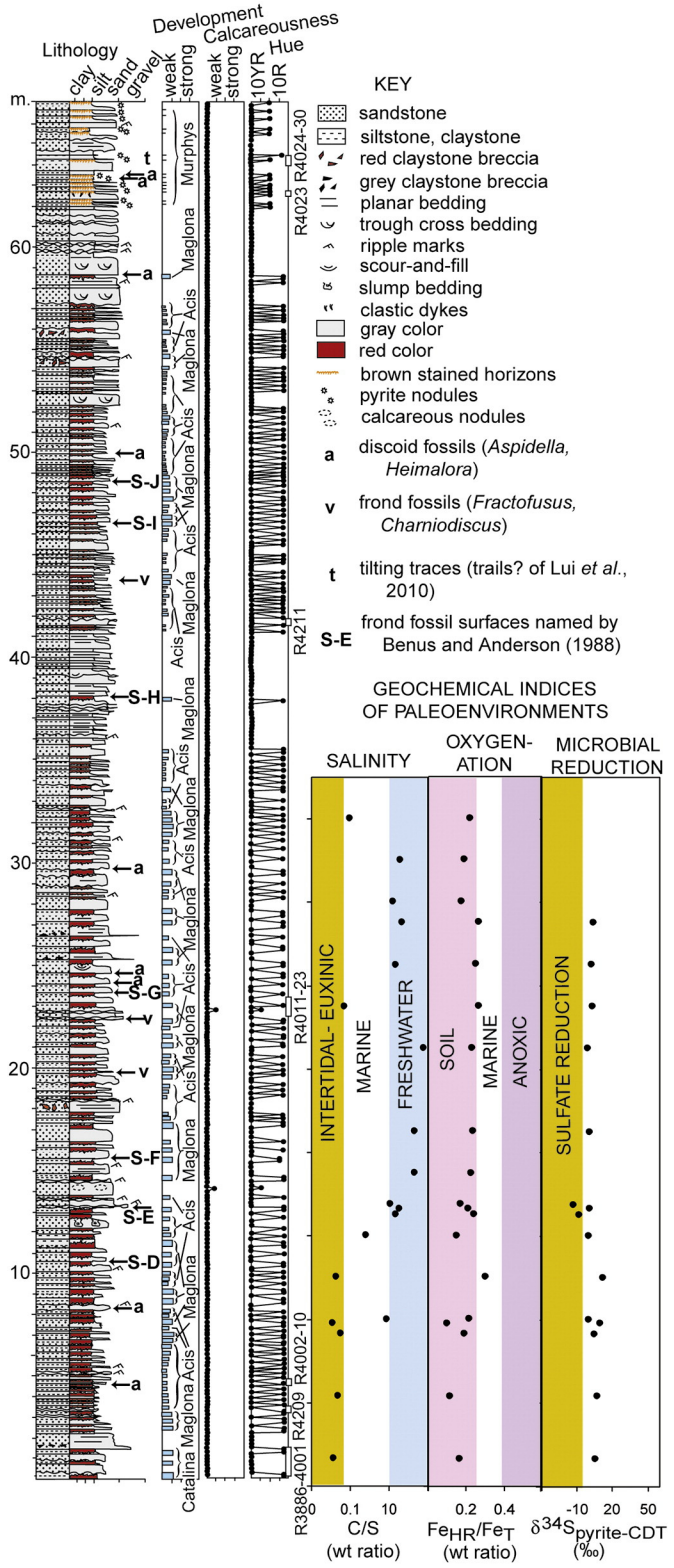

Fig. 3. Measured section of the Mistaken Point Formation (after Retallack, 2014b) through the lettered fossiliferous horizons (D–J) recognized by Benus (1988) at Mistaken Point, with selected paleoenvironmental proxy data for part of the section (Canfield et al., 2007), on fields by modern behavior of C/S ratios (Berner and Raiswell, 1984; Raiswell and Berner, 1986), Fe_{HRT}/Fe_{TOT} ratios (Ku et al., 2008) and pyrite isotopic composition (Canfield et al., 2007, 2010).

and for ferrous iron using Pratt titration by ALS Chemex of Vancouver, BC (Retallack, 2014a). Bulk density was determined by the clod method using paraffin (Retallack, 1997). Consumable specimens (R3925-4079) are curated within the Condon Collection of The Museum of Natural and Cultural History of the University of Oregon, Eugene (G.J. Retallack, director), and archival polished slabs (G149-G176) in collections of The Rooms (provincial museum), St. John's, Newfoundland (N. Djan-Chekar, curator).

Newfoundland beds were also compared with known Phanerozoic turbidites studied in the field and by means of polished slabs, from the following localities: middle Ediacaran (584 Ma), upper Mall Bay Formation, St Marys, Newfoundland, Canada (Retallack, 2013a; N46.91933° W53.59828°); Late Ordovician (Sandbian, 455 Ma), Malongulli Formation, Millamolong, New South Wales, Australia (Stevens, 1957; Percival and Glen, 2007; S33.585738° E148.973131°); middle Silurian (Wenlockian, 430 Ma), Trail Creek Formation, 15 km east of Sun Valley, Idaho, USA (Dover et al., 1980; N43.81909° W114.25926°); Early Devonian (Lochkovian, 415 Ma), Waterbeach Formation, Crudine, New South Wales, Australia (Jagodzinski and Black, 1999; S33.04409° E149.52856°), and Oligocene (30 Ma) Mehama Formation, Goshen, Oregon, USA (McClaughry et al., 2010; N44.001294° W123.01423°). Also examined in outcrop, but too clayey and friable to take a polish, were turbidites of the early Eocene Tyee Formation, near Drain, Oregon (Snavely et al., 1964; Ryu, 2007; N43.66158° W123.34034°) and early Eocene, Elkton Formation, near Elkton, Oregon (Weatherby, 1991; Ryu, 2007; N43.60210° W123.62171°). Other outcrops of coastal paleosols and tsunamites were examined in the middle Eocene, Bateman Formation, near Elkton, Oregon (Weatherby, 1991; Ryu, 2007; N43.59774° W123.62929°), and correlative Coaledo Formation at Shore Acres, Oregon (Dott and Bourgeois, 1982; N43.322443° W123.387027°). Polished slabs are curated in the Condon Collection of the Museum of Natural and Cultural History of the University of Oregon.

The distinction between turbidites or tsunamites and paleosols also was attempted by calculating molar ratios for evidence of hydrolysis and other soil-forming processes, by dividing weight percents by molecular weights (Retallack, 1997, 2001). In addition, bulk density was used to calculate gains and losses (mass transfer) of elements in a soil at a given horizon ($\tau_{w,j}$ in moles) from bulk density of the soil (ρ_w in g cm^{-3}) and parent material (ρ_p in g cm^{-3}) and from the chemical concentration of the element in soils ($C_{j,w}$ in weight %) and parent material ($C_{p,w}$ in weight %). Also needed are changes in volume of soil during weathering (strain: $\varepsilon_{i,w}$ as a fraction), estimated from an immobile element in soil (such as Ti used here) compared with parent material ($\varepsilon_{j,p}$). The relevant equations (Brimhall et al., 1992) are given in Table 1. The expectation is that well-drained paleosols would show negative strain and mass transfer, but poorly drained paleosols, turbidites, and tsunamites would show little or positive strain and mass transfer (Retallack, 2001).

4. Comparative sedimentology

Genuine turbidites, tempestites, tsunamites, and intertidal to supratidal paleosols are briefly documented and discussed in the following paragraphs in order to establish differentiating criteria. Although very different in origin, these various kinds of graded beds can appear superficially similar and can all be found in thick forearc basin successions, as envisaged for the Conception Group of Newfoundland (Retallack, 2014a). These expectations are then compared directly with individual Ediacaran beds in Newfoundland, in order to infer their genesis.

4.1. Turbidites

In the field and polished slabs, turbidites show characteristic normal grading by grain size in intertidal (Fig. 6A), graptolite-bearing deep marine (Fig. 6B–D), foraminifera-bearing deep marine (Fig. 7A, B), and shallow lacustrine facies (Fig. 6E). There is great variation of relative thickness of coarse and fine parts of these graded beds, in part due to differences in their paleoenvironments. Thick fine tails were more

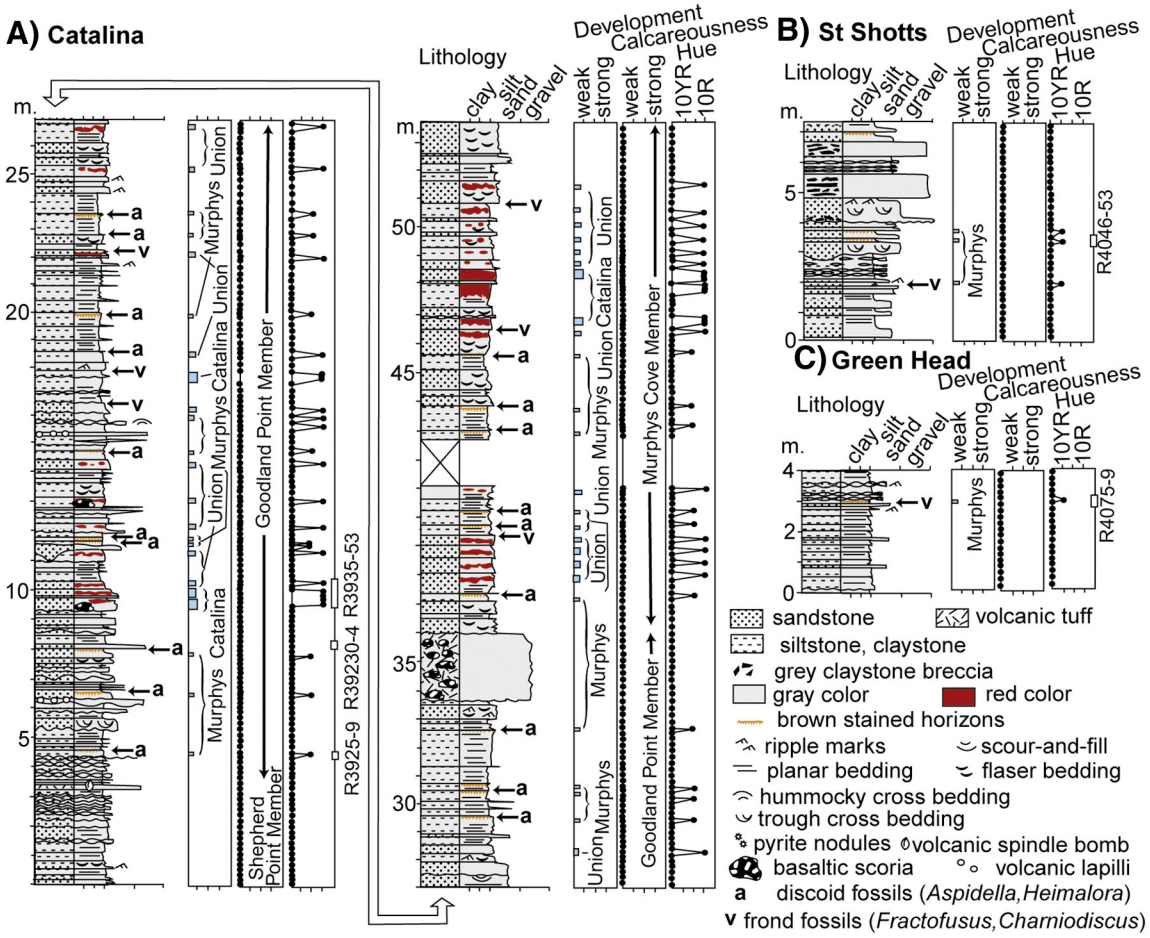

Fig. 4. Measured sections of the Mistaken Point Formation at Murphy's Cove (A), St Shotts (B), and Green Head (C).

common in turbidites considered deep water (Jagodzinski and Black, 1999; Ryu and Niem, 1999) than those thought to have been deposited in shallow water (McClaughry et al., 2010; Retallack, 2013a). Turbidites share gray color, even when stained orange or yellow by weathering in modern outcrop (Fig. 6B and D). Grain size grading also persists when partly destroyed by burrowing (Fig. 6C). Ripple marks and washouts reveal traction currents during waning phases of turbidite current (Figs. 6A–D and 7A, B). Also common are erosional bed bases showing scours and lensing (Fig. 6A, B, and D). These various observations correspond well with other descriptions of turbidite facies and processes (Bouma, 1962; Ludlam, 1974; Talling et al., 2012).

4.2. Tempestites

Tempestites are event deposits of storms with sand to breccia grain size and a variety of sedimentary structures revealing high energy deposition (Seilacher, 1982). A key sedimentary structure is hummocky cross stratification formed by storm wave interference creating broad domal structures (Fig. 7E). The low domes rise from a planar-bedded base and are always in cosets. Convolute lamination, claystone breccias, fossil shells, and megaripples are commonly associated with hummocky stratification (Dott and Bourgeois, 1982). The sudden onset of violent from still conditions is revealed by shales or burrows above and below the hummocky coset (Fig. 7E). These observations of hummocky stratification are similar to other occurrences (Dashtgard et al., 2009), but single-set smaller features have been misidentified as hummocky stratification elsewhere (Higgs, 2011; Tarhan et al., 2015).

4.3. Tsunamites

Tsunamites are best known within Holocene tidal flats and marshes in Oregon (Atwater et al., 1992; Atwater and Hemphill-Haley, 1997) and Chile (Cisternas et al., 2005), where they can often be attributed to known subduction zone earthquake events. They are clean, white, planar-bedded, sand beds, 5–20 cm thick within sequences of peat and claystone, including stumps and leaf litter of buried coastal soils. Comparable thin, planar- to wavy-bedded sands were also left on fields and streets by the 2011 Tohoku-oki tsunami (Szczuciński et al., 2012).

Tsunamites are little known in deep time but are well exposed in Eocene marine rocks near Elkton, Oregon (Fig. 7A, B). The Bateman Formation shows common thin tsunamites separating intertidal siltstones with estuarine fossil crabs (*Raninoides lewisianus*) and clams (*Brachidontes cowlitzensis*, *Nuculana washingtonensis*) and carbonaceous root traces (Weatherby, 1991). The tsunamites are thin sandstones with sharp tops and bottoms, washed-out ripples to parting lineation, and plane bedding. They stand out as the most clearly bedded horizons within massive pyritic siltstones, thoroughly bioturbated by root traces and burrows. The tsunamite grain size does not grade into intervening massive siltstones, which appear to be bioturbated suspension deposits.

4.4. Intertidal and supratidal paleosols

Intertidal siltstones of the Eocene Bateman Formation of Oregon (Fig. 7C–D) contain not only fossil estuarine crabs and clams but also carbonaceous root traces (Weatherby, 1991), so were intertidal

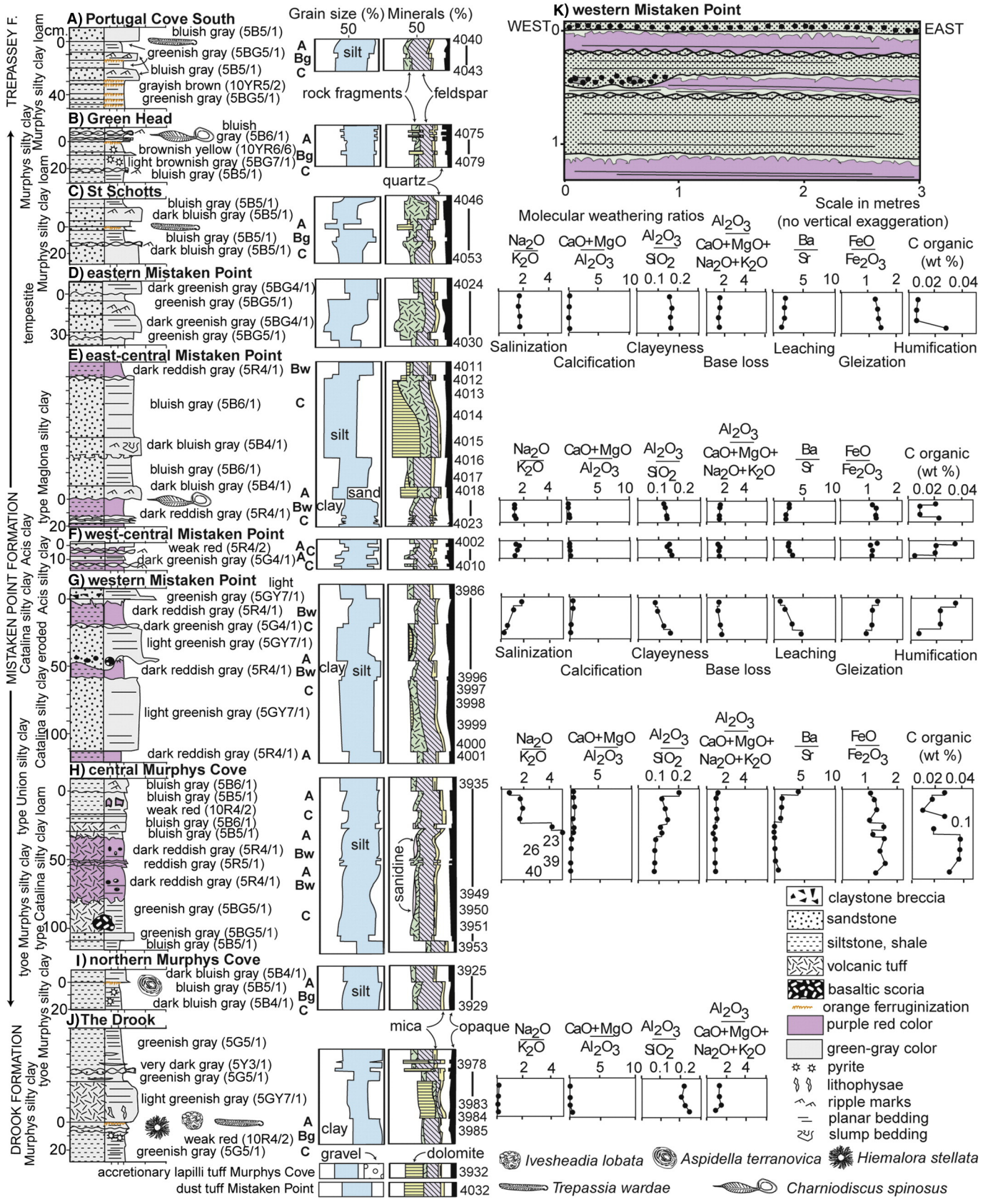

Fig. 5. Grain size and mineral (from point counting) and chemical composition (from X-ray fluorescence) of paleosols, tuffs, and tempestites of the Conception Group of Newfoundland, with field sketch (upper right) of paleosol erosion at 0–1.5 m, Mistaken Point. Molar weathering ratios are designed to reveal degree of common soil-forming reactions, such as base loss (Retallack, 1997).

Table 1
Transfer functions used to interpret Ediacaran paleosols.

Equation	Variables	Coefficient of variation (R^2)	Standard error	Reference
$\tau_{j,w} = \left[\frac{\rho_w \cdot C_{j,w}}{\rho_p \cdot C_{j,p}}\right]\left[\varepsilon_{i,w} + 1\right] - 1$	$\tau_{w,j}$ (mole fraction) = mass transfer of a specified (j) element in a soil horizon (w); ρ_w (g cm^{-3}) = bulk density of the soil; ρ_p (g cm^{-3}) = bulk density of parent material; $C_{j,w}$ (weight %) = chemical concentration of an element (j) in a soil horizon (w); $C_{p,w}$ (weight %) = chemical concentration of an element (j) in the parent material (p): $\varepsilon_{i,w}$ (mole fraction) = strain due to soil formation	Not applicable to mass balance equation	Not applicable to mass balance equation	Brimhall et al., 1992
$\varepsilon_{i,w} = \left[\frac{\rho_p \cdot C_{i,p}}{\rho_w \cdot C_{i,w}}\right] - 1$	$\varepsilon_{i,w}$ (mole fraction) = strain of a soil horizon (w) with respect to a stable chemical constituent (i); ρ_w (g cm^{-3}) = bulk density of a soil horizon; ρ_p (g cm^{-3}) = bulk density of parent material; $C_{i,w}$ (weight %) = chemical concentration of stable element (i) in a soil horizon (w); $C_{p,w}$ (weight %) = chemical concentration of stable element (i) in the parent material (p)	Not applicable to mass balance equation	Not applicable to mass balance equation	Brimhall et al., 1992
$T = 0.21I - 8.93$	T (°C) = mean annual palaeotemperature; I (mole fraction) = chemical index of weathering ($I = \frac{100Al_2O_3}{(Al_2O_3+CaO+Na_2O)}$)	0.81	±0.5 °C	Óskarsson et al., 2012)
$P = 221e^{0.0197I}$	P (mm) = mean annual precipitation; I (mole fraction) = chemical index of weathering ($I = \frac{100Al_2O_3}{(Al_2O_3+CaO+Na_2O)}$)	0.72	±182 mm	(Sheldon et al., 2002)

paleosols of mangrove vegetation. These paleosols are gray colored, with local high chroma red mottles and seams, weak relict bedding, and common subsurface pyrite nodules and framboids. Comparable drab, red-mottled intertidal paleosols, and red-green-mottled supratidal paleosols are well known from the Miocene (Retallack and Kirby, 2007) and Cretaceous (Retallack and Dilcher, 2012). Pyrite, red mottles, and relict bedding also characterize early Cambrian (Retallack, 2013c) and Ediacaran (Retallack, 2014b, d) intertidal paleosols, although these are geologically too old for root traces and large shells. Intertidal paleosols are easily overlooked because they retain relict bedding and estuarine fossils and lack the dominantly red color, strong soil structure, and geochemical and mineralogical horizon differentiation of well-drained paleosols (Retallack, 1997, 2001).

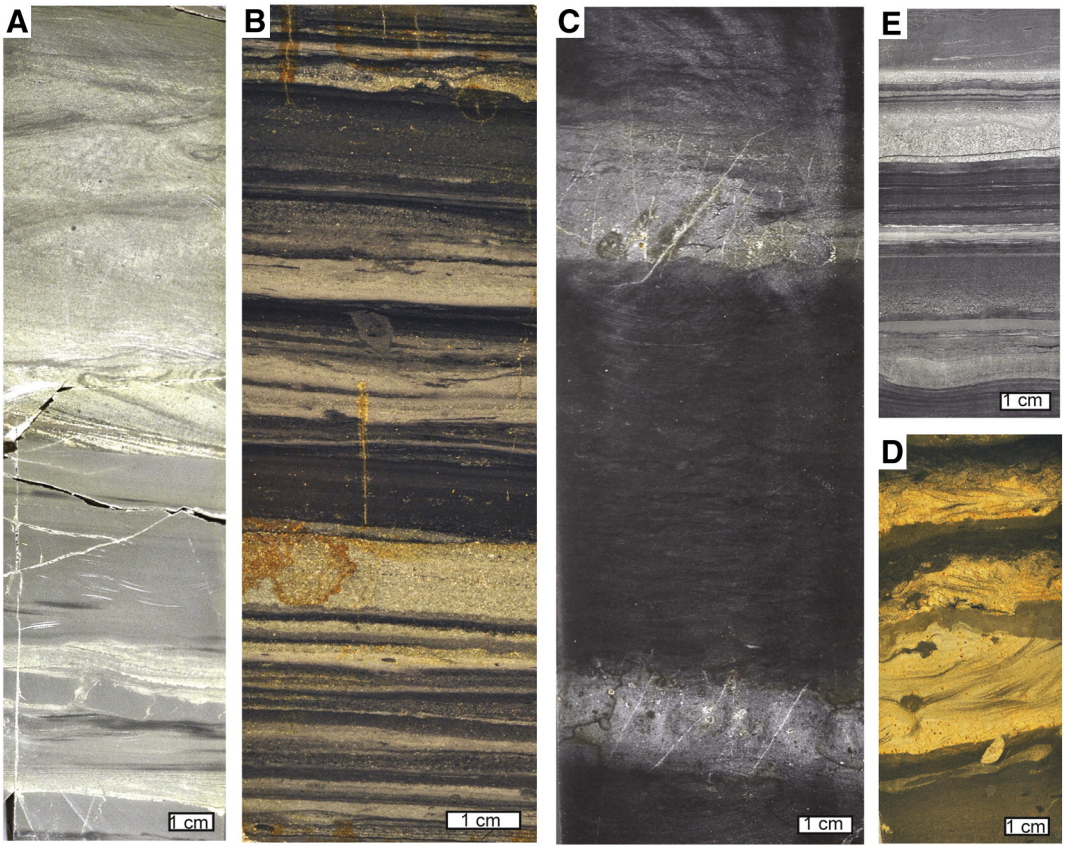

Fig. 6. Polished slabs of intertidal (A), deep marine (B–D), and lacustrine (E) graded beds. A, middle Ediacaran (584 Ma), upper Mall Bay Formation, St Marys, Newfoundland, Canada; B, Late Ordovician (Sandbian, 455 Ma), Malongulli Formation, Millamolong, New South Wales, Australia; C, middle Silurian (Wenlockian, 430 Ma), Trail Creek Formation, 15 km east of Sun Valley, Idaho, USA; D, Early Devonian (Lochkovian, 415 Ma), Waterbeach Formation, Crudine, New South Wales, Australia; E, Oligocene (30 Ma) Mehama Formation, Goshen, Oregon, USA. Specimens are curated in the Condon Collection of the Museum of Natural and Cultural History of the University of Oregon: R4171B (A), R5061A (B), R4164B (C), R5056A (D), R4163B (E).

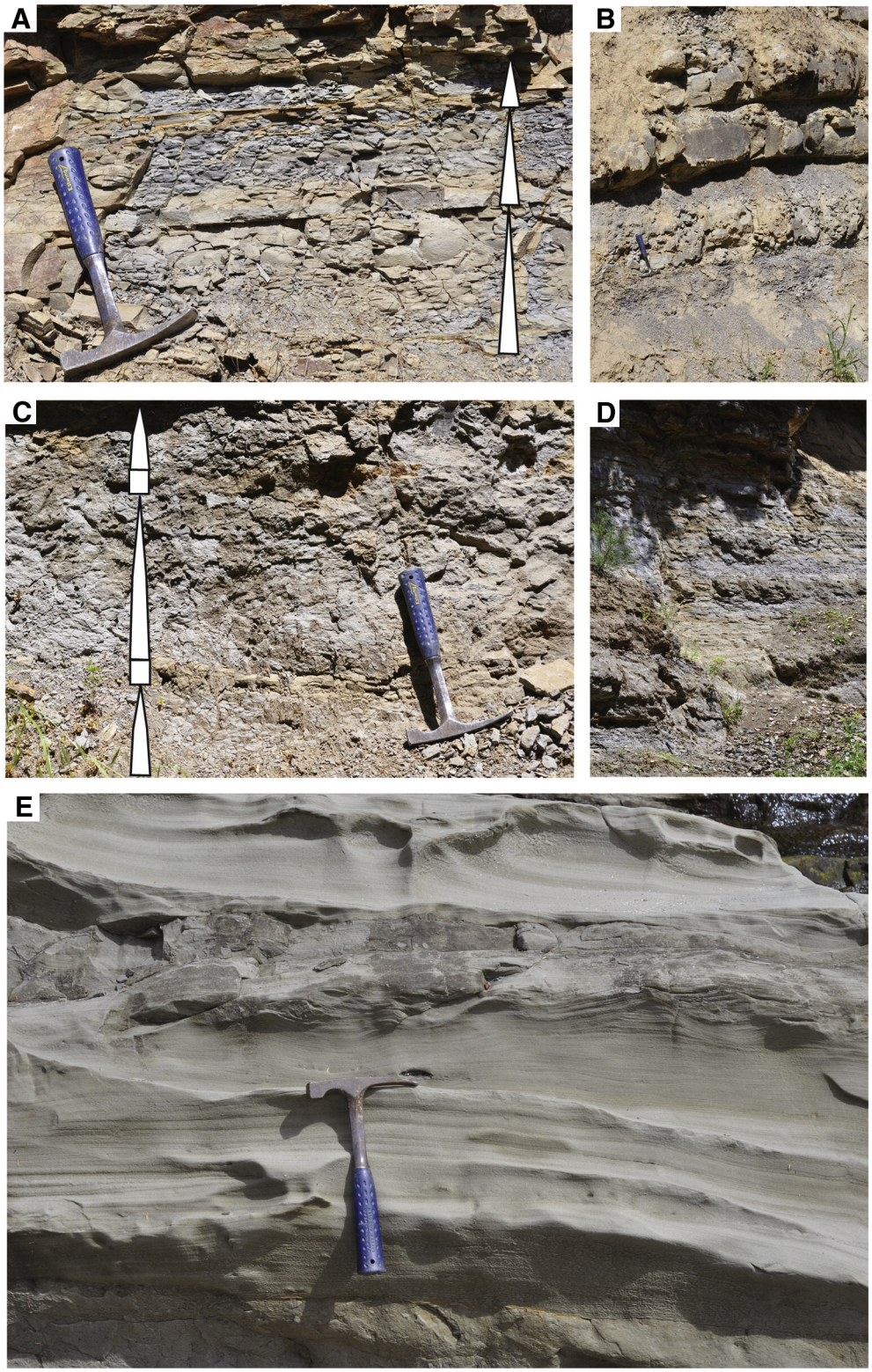

Fig. 7. Field photographs contrasting turbidites in the Eocene, Elkton Siltstone (A), and Tyee Formation (B), near Elkton (A) and Drain (B), with tsunamites and intertidal pyritic paleosols in the middle Eocene, Bateman Formation (C–D), near Elkton, Oregon, as well as hummocky cross stratification from the Eocene Coaledo Formation at Simpson's Beach, Oregon (E). Tsunamite sandstones have sharp tops and bottoms, intertidal paleosols show grading only near the surface, but turbidites are graded throughout. Hammers for scale are 25 cm long.

4.5. Forearc basin successions

The Elkton (900 m thick), Bateman (900 m), and Lower Coaledo (300 m) formations are the upper 2.1 km of the Tyee Basin, a 9.2 km thick forearc basin sequence of Eocene age in the southern Oregon Coast Range (Dott and Bourgeois, 1982; Heller et al., 1985; Ryu and Niem, 1999). Much of this great thickness is turbidites and submarine fans (Fig. 7A, B), but only the upper 1.2 km formed on continental shelf to shorefaces with hummocky bedding and intertidal deposits (Fig. 7C–E). Most forearc basins have thin intervals of shallow

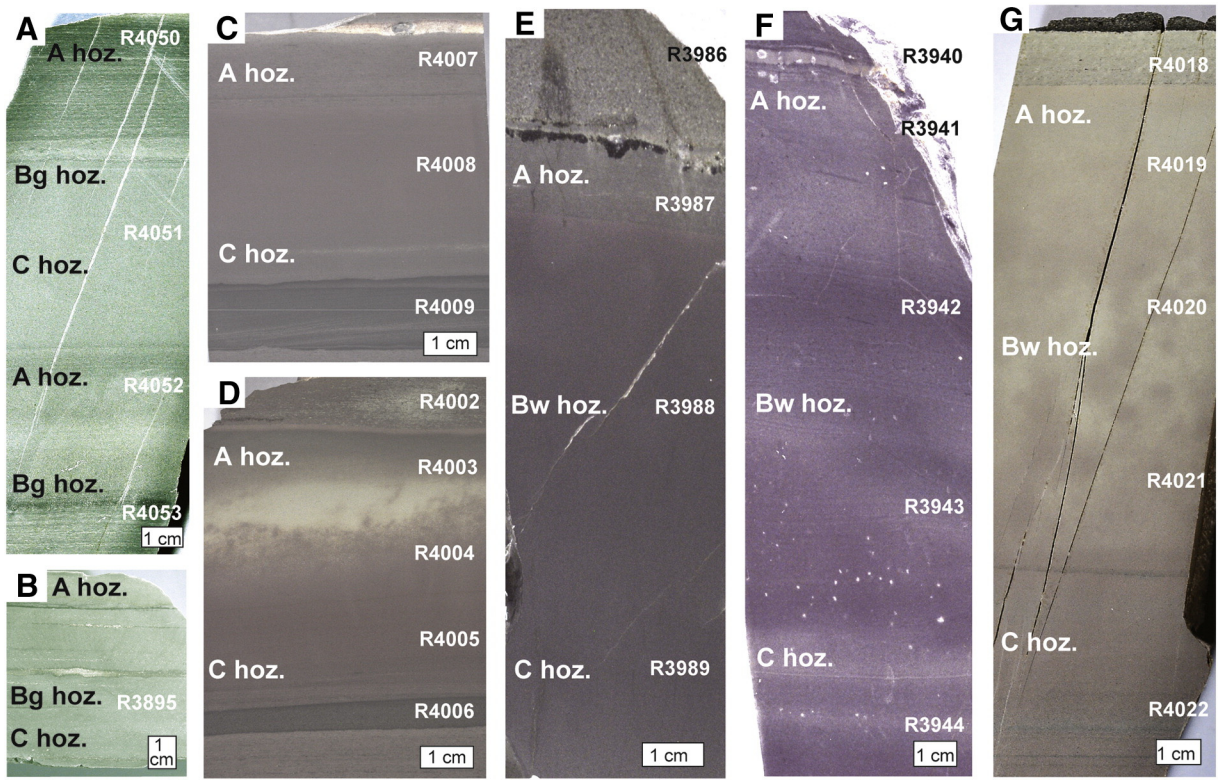

Fig. 8. Polished slabs of Ediacaran paleosols from the Mistaken Point (A, C–G) and Drook Formation (B) of Newfoundland showing variation in redox (red versus green) and destruction of bedding (laminated versus massive): (A) Murphy's paleosol at 2.0 m., St Shotts; (B) Murphy's paleosol below tuff at Pigeon Cove; (C) Acis paleosol at 9.7 m, Mistaken Point; (D) Acis paleosol at 9.8 m, Mistaken Point; (E) Catalina paleosol at 1.3 m, Mistaken Point; (F) Catalina paleosol at 9.6 m., Murphy's Cove; (G) Maglona paleosol at 22.5 m, Mistaken Point;. Specimen numbers in The Rooms, St. John's, are NFM G-174 (a), NFM G-157 (b), NFM G-163 (c), NFM G-162 (d), NFM G-159 (e), NFM G-154 (f), NFM G-167 (g). Designations of A and B horizons are interpretations from the terminology of soil science (Retallack, 2001).

(intertidal) facies but great thicknesses of deep (turbidite) facies (Ito and Katsura, 1992; Takashima et al., 2004). The Conception Group of Newfoundland has a similar ratio of thin shallow-water and thick deep-water facies (Retallack, 2014b).

4.6. Glacioeustatic sea level changes

Forearc basins not only show close geographic juxtaposition of coastal facies and deep trench sedimentary facies, but steep gradients and facies changes record fluctuation in sea level with waxing and waning of ice caps. Deep-water turbidites of the Elkton Formation correlate with a middle Eocene high sea level, but tsunamites of the Bateman Formation and coal seams of the Coaledo Formation correlate with a late middle Eocene 70 m sea level fall (van Sickel et al., 2004). A late Eocene high stand is reflected in deeper water shales of the upper Coaledo Formation, but marine regression from the Oligocene in Oregon corresponds with growth of the Antarctic ice sheet (Zachos et al., 2001). The Conception Group of Newfoundland also records profound glacioeustatic regression during the Gaskiers Glaciation (Retallack, 2013a).

4.6. Comparisons with Mistaken Point Formation of Newfoundland

Graded beds of the Mistaken Point Formation (Fig. 8) have been interpreted widely as turbidites (Anderson and Misra, 1968; Misra, 1971; Clapham et al., 2003; Narbonne et al., 2005; Hofmann et al., 2008; Liu et al., 2015), but these red silty beds bear little resemblance to turbidites (Figs. 6 and 7A, B). Siltstone beds in Newfoundland do not grade upwards into shale or downwards into sandstone but have sharp tops as well as bottoms (Fig. 8D, G). Much of the appearance of grading by grain size (Fig. 8) is loss of bedding upwards (Fig. 5). The thin intervening sandstone beds have planar bedding and sharp tops and bottoms better interpreted as tsunamites (Retallack, 2014b), like those of the Bateman Formation of Oregon (Fig. 7C–D) and the 2011 Tohoku-oki tsunami (Szczuciński et al., 2012). The Newfoundland red beds have abundant silt-size grains (Fig. 5), and very little clay, unlike turbidites and other deep-sea oozes (Fig. 6). Clayey beds in Newfoundland are gray, pyritic, and ungraded (Fig. 5). Sandstone beds in Newfoundland with hummocky stratification, convolute lamination, and megaripples (Fig. 5E; Retallack, 2014a, Fig. 4F) appear to be tempestites (Dalrymple et al., 1999), like those where hummocky stratification was defined in the lower Coaledo Formation of Oregon (Fig. 7E). Tempestite beds are not common in the Coaledo or Mistaken Point Formation, but the Bateman (Fig. 7C, D) and Mistaken Point Formations (Figs. 3 and 4A) have many successive tsunamite beds.

Also comparable with the Bateman Formation and Tohoku-oki sediments, polished slabs of Newfoundland red and grey siltstones revealed a variety of features of paleosols (Fig. 8). Some of the beds are gray and pyritic with relict bedding (Fig. 8A, B), like intertidal paleosols (Fig. 7C, D), but others are red and mottled like intermittently drained and oxidized coastal paleosols (Fig. 8C, G). In all cases, the uppermost portion of the purple siltstones are less distinctly laminated than the lower portions, a characteristic feature of soil disruption (Retallack, 2014a). Degree of surficial disruption was minimal in gray siltstones (Fig. 8A, B), and some thin red siltstones (Fig. 8C, D), but more marked in thick red siltstones (Fig. 8E, G), comparable with variations attributed to varying time available for soil formation in paleosols (Retallack, 2014a).

Disruption of primary lamination in Newfoundland Ediacaran paleosols is accompanied by drab mottles (Fig. 8D, F), comparable with drab surfaces and drab-haloed filament traces of other Ediacaran paleosols (Retallack, 2013a, b) in showing little significant iron mobilization (Fig. 5). Disruptions nearest the surface are by the basal stalks of fossil vendobiont fronds (Fig. 9B), but deeper within the profiles are finer filaments of thinner stalks (Fig. 9B) and disruptions on the micron

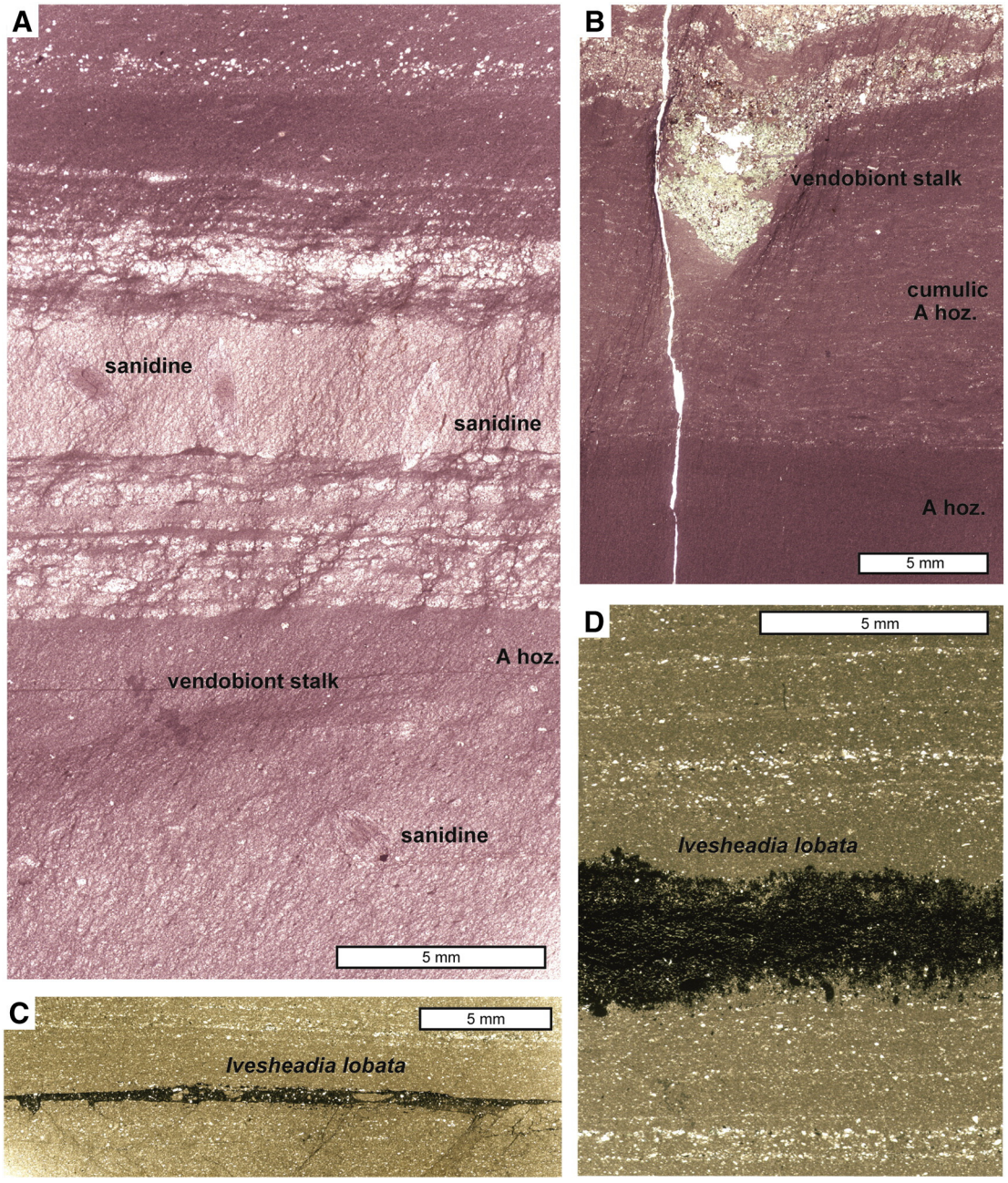

Fig. 9. Photomicrographs of vendobiont fossils in place of growth from the Mistaken Point (A, B) and Drook Formations (C, D) of Newfoundland: A, oblique vendobiont stalk and euhedral sanidine crystals (labeled) in A horizon of Catalina paleosol at 9.6 m., Murphy's Cove; B, stalk of unidentified frond (*Charnia* or *Charniodiscus*) through cumulic ash addition to Catalina paleosol at 1.3 m, Mistaken Point; C, D, tubular interior stucture of *Ivesheadia lobata* from beneath tuff in Drook Formation at Pigeon Point. All images are scanned from slides cut vertical to bedding and oriented with upper side to top. Sample numbers in Museum of Natural and Cultural History of the University of Oregon are R3940 (A), R3987 (B), R3984 (C), R3985 (D).

scale of rope-forming bacteria (Retallack, 2014a). Drab-haloed filament traces are widespread in paleosols of Ediacaran and Cambrian age and are attributed to microbial burial gleization of organic matter (Retallack, 2008, 2013a–c).

Mineral and chemical variation within these red siltstones is compatible with terrestrial weathering, rather than marine diagenesis (Fig. 5). In most cases, both alkali and alkaline earth elements are depleted toward the surface, as expected for hydrolytic weathering (Retallack, 1997). However, alumina enrichment is modest and does not outstrip desilication. These trends were also detected in dacitic volcanic ash of the Mistaken Point and Drook Formation, which showed surprising loss of silica for what appeared to be fresh ash in the field (Retallack, 2014a). Loss of silica may be due to devitrification of volcanic glass, which is very scarce in thin sections (Retallack, 2014a). Ash-dusted Catalina and Union pedotypes fail to show grading expected under water (Retallack, 2014a) and show varied abundance of alkali and alkaline earth elements because of the sprinkling of sanidine phenocrysts (Fig. 5). They are nevertheless red with hematite and have ferrous–ferric iron ratios near unity (Fig. 5), like intermittently oxidized and gleyed paleosols (Retallack and Dilcher, 2012). Gray beds of the Mistaken Point Formation have pyritic horizons below the surface, like soils of marine-influenced intertidal and supratidal flats (Altschuler et al., 1983; Patching, 1987; Retallack and Dilcher, 2012). Such patterns indicate hydrolytic pedogenesis in a coastal environment interrupted by additions of ash and local groundwater stagnation and pyritization.

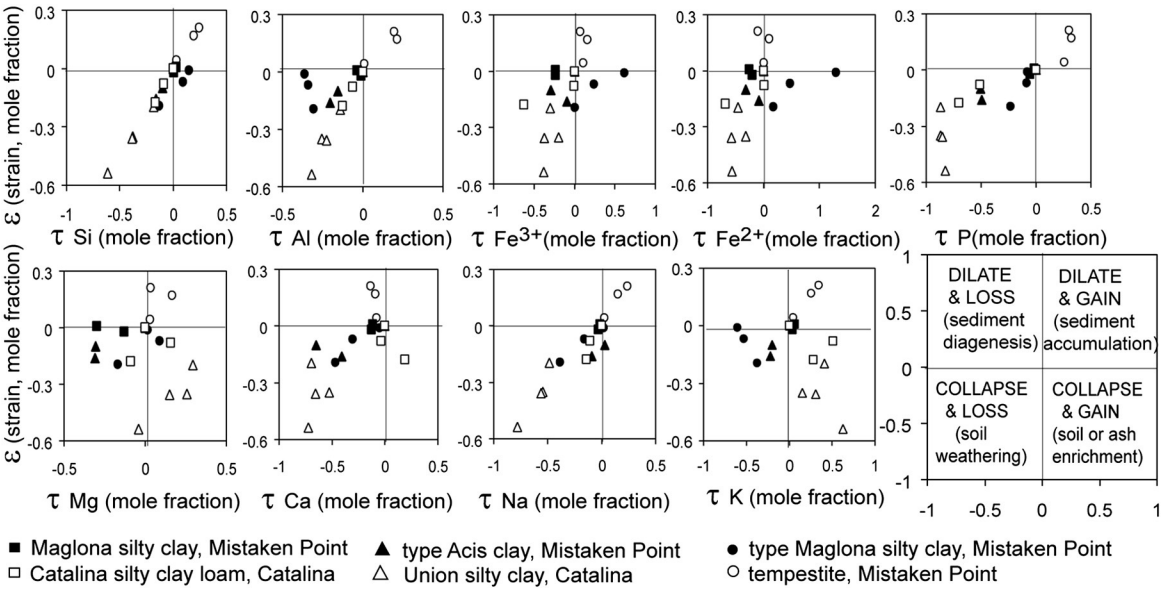

Fig. 10. Mass balance geochemistry of paleosols (lower quadrats) and a tempestite (upper right quadrat) of the Mistaken Point Formation of Newfoundland, including estimates of strain from changes in an element assumed stable (Ti) and elemental mass transfer with respect to an element assumed stable (Ti). Zero strain and mass transfer is the parent material lower in the profile: higher horizons deviate from that point due to soil formation or sedimentation as indicated in key to lower right (Brimhall et al., 1992).

Terrestrial weathering is especially revealed by base cation and volume loss in chemical mass balance of the red siltstone beds because soil formation is a process of nutrient depletion (negative mass transfer and strain in Fig. 10). In contrast, sedimentation without subsequent weathering is a process of adding of both cations and volume, as in event beds, such as the tempestite of Fig. 10, showing positive mass transfer and strain. Furthermore, strong loss of phosphorus in the paleosols, but not sedimentary beds (Fig. 10), is evidence of microbial activity within the paleosols because microorganisms contribute ligands to mobilize phosphorus from apatite (Neaman et al., 2005).

Although bed-scale observations of the Mistaken Point Formation (Figs. 5 and 8–10) and Gaskiers Formation (Retallack, 2013a), reveal a variety of paleosols, other parts of the Conception Group show graded bedding comparable with turbidites, especially in the Fermeuse, Briscal, lower Drook, and Mall Bay Formations (King, 1988; Retallack, 2014a). The 7.4 km thickness of Conception, St. John's and Signal Hill groups (Fig. 2) is thus similar to comparably thick sequences of the Tyee Basin of Oregon (Heller et al., 1985; Ryu and Niem, 1999) and comparable forearc basins elsewhere (Ito and Katsura, 1992; Takashima et al., 2004) in showing both deep-sea turbidites and paleosols at different stratigraphic levels.

Red beds of the Mistaken Point Formation represent a sea level drop because they are underlain and overlain by marine facies (Retallack, 2014a). This marine regression was glacioeustatic because the same age as the Fauquier Glaciation, named for a glacial diamictite and a 'cap carbonate' of the Fauquier Formation in Virginia, below Catoctin Volcanics dated at 571 ± 1 Ma by zircon U–Pb (Hebert et al., 2010). The Fauquier Glaciation was 567 ± 6 Ma in age from the interpolated age of paleocanyons created by sea level drop of 700 m in the Wonoka Formation of South Australia (Retallack et al., 2014). This age of the Fauquier Glaciation is indistinguishable from the 565 ± 3 Ma age by zircon U–Pb of the Mistaken Piont Formation (van Kranendonk et al., 2008). The best known Ediacaran glacioeustatic sea level drop was during the Gaskiers Glaciation, significantly older at between 582.4 ± 0.5 Ma and 583.7 ± 0.5 Ma by zircon U–Pb in the upper and lower parts of the Gaskiers Formation, respectively (van Kranendonk et al., 2008). The Gaskiers Formation of Newfoundland included a terrestrial moraine interbedded with paleosols and is overlain and underlain by marine gray facies (Retallack, 2013a).

Table 2
Definition and identification of paleosols in the Mistaken Point Formation.

Pedotype	Derivation	Diagnosis	US taxonomy (Soil Survey Staff, 2010)	FAO world map (Food and Agriculture Organization, 1974)	Australian classification (Isbell, 1996)
Acis	S.S. Acis shipwreck August 3, 1901	Thin drab-mottled surface (A) over red bedded siltstone (C)	Fluvent	Eutric Fluvisol	Lutic Rudosol
Catalina	Town of Catalina	Thin drab-mottled surface with scattered sanidine crystals (A) over thick red siltstone (Bw) and red bedded siltstone (C)	Eutrudept	Eutric Cambisol	Red-Orthic Tenosol
Maglona	Schooner Maglona shipwreck September 2, 1887	Thin drab-mottled surface (A) over red massive siltstone (Bw) and red bedded siltstone (C)	Eutrudept	Eurtric Cambisol	Red-Orthic Tenosol
Murphy's	Murphy's Cove, near Port Union	Thin carbonaceous gray shaley silt (A) over gray sheley silt with pyrite framboids and stringers (By)	Sulfaquent	Thionic Fluvisol	Intertidal Hydrosol
Union	Fishing village of Port Union	Thin drab-mottled surface with scattered sanidine crystals (A) over thick red siltstone with relict bedding (C)	Fluvent	Eutric Fluvisol	Lutic Rudosol

Table 3
Interpretation of paleosols in the Mistaken Point Formation.

Pedotype	Palaeoclimate	Organisms	Palaeotopography	Parent material	Time of soil formation
Acis	Humid (975 ± 182 mm MAP) cool temperate (8.8 ± 0.7 °C MAT)	*Aspidella terranovica*, *Bradgatia linfordensis*, *Charnia grandis*, *Charniodiscus spinosus*, *Fractofusus andersoni*, *Ivesheadia lobata*, *Primocandelabrum heimaloranum*	Well-drained estuary margin	Rhyodacitic reworked tuff	10–100 yr
Catalina	Humid (>633 ± 182 mm MAP) cool temperate (>8.1 ± 0.7 °C MAT)	*Aspidella terranovica, Charnia antecedens*, *C. masoni*, *C. grandis*, *Charniodiscus arboreus, Fractofusus misrai, Hadryniscala avalonica, Hadyrnichorde catalinica, Heimalora stellaris, Ivesheadia lobata, Primocandelabrum heimaloranum, P. sp.*	Well-drained coastal floodplain	Sanidine tuff	1000–5000 yr
Maglona	Humid (1065 ± 182 mm MAP) cool temperate (8.8 ± 0.7 °C MAT)	*Aspidella terranovica, Beothukis mistakenensis, Bradgatia linfordensis, Fractofusus andersoni, F. misrai, Charnia masoni, Charniodiscus procerus, C. spinosus, Hapsidophyllas flexilis, Ivesheadia lobata, Parviscopa bonavistensis, Pectinifrons abyssalis, Primocandelabrum heimaloranum, Thectardis avalonensis*	Well-drained coastal floodplain	Rhyodacitic reworked tuff	1000–5000 yr
Murphy's	Not diagnostic of climate	*Aspidella terranovica, Avalofractus abaculus, Charnia antecedens, Charniodiscus arboreus, C. spinosus, Heimalora stellata, Ivesheadia lobata, Thectardis avalonensis, Trepassia wardae*	Intertidal flats	Rhyodacitic silty clay	10–100 yr
Union	Humid 909 ± 182 mm MAP) cool temperate (9.9 ± 0.7 °C MAT)	*Aspidella terranovica, Bradgatia linfordensis, Charnia antecedens, C. masoni, C. grandis, Charniodiscus spinosus, Fractofusus misrai, F. andersoni, Heimalora stellaris, Ivesheadia lobata*	Well-drained estuary margin	Sanidine tuff	10–100 yr

5. Paleoecology of the fossils

5.1. Fossil preservation

An evocative feature of Newfoundland Ediacaran fossils is the appearance that they were knocked down where they grew, as indicated by consistently oriented holdfasts, distinct tiering, and regular spacing of the fossils (Clapham et al., 2003). Firm attachment by distributed systems of organic tubules was confirmed in petrographic thin sections intersecting vertical stalks (Fig. 9A, B) and fine tubules below other fossils (Fig. 9C, D). Specimens in gray shale are pyritized (Fig. 9C, D), but others in red beds are not pyritized and show only remnant organic matter (Fig. 9A, B). Pyritized specimens (Fig. 9C, D) are permineralized, with pyrite filling cell lumens (Retallack, 2011), rather than pyritic surficial encrustations, or "death masks" of Gehling (1999).

Ediacaran fossils from Newfoundland are thus unlike fossils found in turbidites, which are mainly trace fossils scattered through accreting shaley bed tops and truncated by scouring of the next turbidite, because shells are poorly preserved below calcium carbonate compensation depth, and the deep sea is too oligotrophic for common large organic fossils (Sutcliffe et al., 1999). Newfoundland Ediacaran fossil beds are more like miniature fossil forests (DiMichele and Falcon-Lang, 2011), or gardens of the ancient Roman city of Pompeii (Jashemski, 1979). Burial by ash has commonly been envisaged for preservation of the Newfoundland Ediacaran fossils (Clapham et al., 2003), but petrographic examination of covering sandstone has shown that only a few fossil assemblages (5 of 48 examined) were buried by primary pyroclastic ashes (Figs. 3 and 4). Most fossils were buried by redeposited volcaniclastic (epiclastic) sandstone, which lacks shards or euhedral crystals of primary airfall (Retallack, 2014a). Like deposits of the Tohoku-oki tsunami of March 11, 2011 (Szczuciński et al., 2012) and Holocene paleotsumani beds in Oregon (Peters et al., 2007), these epiclastic sands have a sharp top and bottom and flattened vegetation of the buried soil with little uprooting. Such buried plants in growth position ("ghost forests") have been critical to reconstructing Holocene tsunami history (Peters et al., 2007). Tsunami deposits also have outsize ripup clasts, internal parting lineations, and subtle normal and reverse grading of sand and silt (Peters et al., 2007; Szczuciński et al., 2012), also seen in the sandstone beds of Mistaken Point (Retallack, 2014a).

5.2. Fossiliferous paleosols

Five distinct kinds of paleosols can be recognized in the Mistaken Point and Drook Formation and are named as pedotypes from nearby towns and shipwrecks (Parsons, 2011) and defined in Table 2. Chemical and petrographic data have been used to interpret each pedotype within three modern soil classifications (Food and Agriculture Organization, 1974; Isbell, 1996; Soil Survey Staff, 2010). Pedotypes are the basis for paleoenvironmental interpretations of the paleosols (Table 3).

Ediacaran paleoenvironments of Newfoundland can be interpreted from these paleosols by making modern comparisons (Table 3) and quantifying climatically sensitive features (Retallack, 2014a). A modern soilscape most like paleosols of the Mistaken Point Formation is map unit Je 11-3a (Eutric Fluvisols) covering 2,227 ha of coastal floodplains of lower Rio Villarico and Rio Tolten near Valdivia, Chile (Food and Agriculture Organization, 1971). Lowland Valdivia supports *Nothofagus* forest and has a humid temperate climate (mean annual temperature of 11 °C; mean annual precipitation of 1630 mm; Veblen and Ashton, 1978). Similar organic and oxidized Holocene paleosols separated by tsunamite sands have been excavated along Rio Maullin 200 km south of Valdivia (Cisternas et al., 2005).

Also supportive of a cool temperate paleoclimate is a transfer function based on modern soils under lichen-tundra of Iceland (Óskarsson et al., 2012). These calculations (Table 1) give temperate mean annual paleotemperatures for paleosols of the Mistaken Point Formation: 11.0 ± 0.4 °C for the Union pedotype, 11.1 ± 0.4 °C for Catalina, 11.5 ± 0.4 °C for type Maglona, 11.2 ± 0.4 °C for another Maglona and 10.9 ± 0.4 °C for Acis. A humid paleoclimate comes from another pedogenic proxy (Sheldon et al., 2002) of chemical index of alteration without potash, which increases with mean annual precipitation. For paleosols of the Mistaken Point Formation, such calculations yield humid mean annual precipitation: 909 ± 182 mm for the Union pedotype, 633 ± 182 mm for Catalina, 1065 ± 182 mm for type Maglona, 1062 ± 182 mm for another Maglona and 975 ± 182 mm for Acis. The estimate for the Catalina paleosol is anomalous due to scattered sanidine crystals (Fig. 9A). These estimates are unlikely to be compromised by high CO_2 because the Mistaken Point Formation is correlative with Fauquier Glaciation and sea level drop (Retallack, 2014a; Retallack et al., 2014). Humid temperate paleoclimate is unremarkable for the kinds of paleosols found (Table 3), and for the putative paleolatitude of S34 ± 8° inferred from paleomagnetic directions of the coeval and nearby Marystown and Harbour Main Volcanics (Pisarevsky et al., 2012). Ediacaran paleoclimate of Newfoundland was thus different from low latitude arid Ediacaran paleoclimate of South Australia (Retallack, 2013b), demonstrating a wide paleoclimatic range for vendobionts.

5.3. Vendobiont paleoecology

Different fossil assemblages vary with differences between the five recognized pedotypes, and may reflect paleoecological zonation and

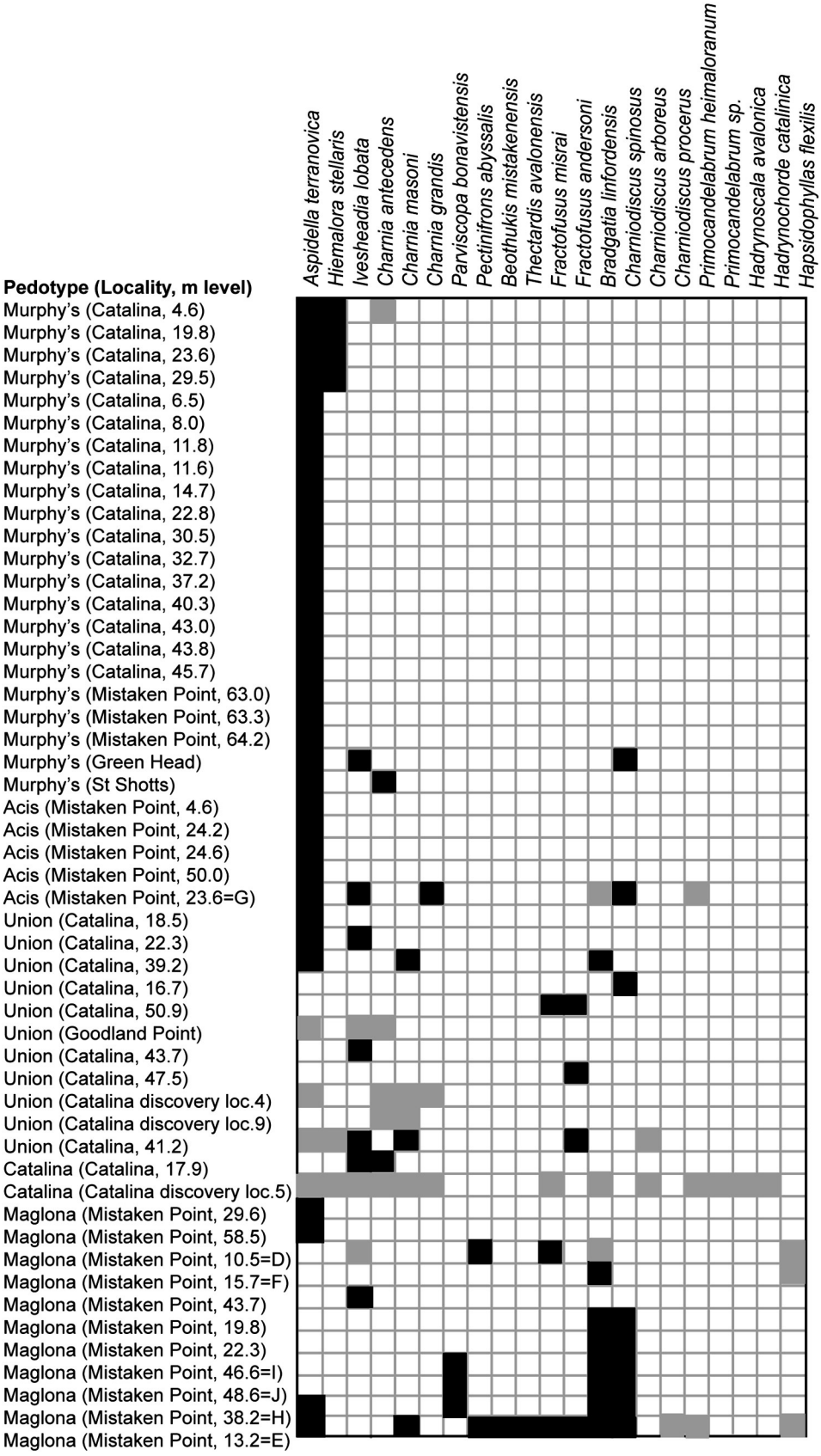

Fig. 11. Phytosociology chart for fossils from paleosols of the Mistaken Point Formation of Newfoundland. Black squares are occurrences recorded in the field. Gray squares include other published accounts of paleosols (O'Brien and King, 2004; Hoffman et al., 2008) and fossil occurrences (Clapham et al., 2003, 2004; Laflamme et al., 2004; Gehling and Narbonne, 2007; Bamforth et al., 2008; Flude and Narbonne, 2008; Hofmann et al., 2008; Bamforth and Narbonne, 2009; Brasier and Antcliffe, 2009; Darroch et al., 2013).

succession. Fossils were observed during fieldwork (black in Fig. 11) on each of the paleosols of the measured sections (Figs. 3 and 4) and inferred from prior publications (grey in Fig. 11, after O'Brien and King, 2004; Laflamme et al., 2004; Clapham et al., 2003, 2004; Gehling and Narbonne, 2007; Hofmann et al., 2008; Bamforth et al., 2008; Flude and Narbonne, 2008; Bamforth and Narbonne, 2009; Brasier and Antcliffe, 2009; Darroch et al., 2013).

Low-diversity (1–2 spp.) assemblages of discoid fossils (*Aspidella* and *Heimalora*) are found largely in Murphy's pedotype gray and pyritic paleosols. The greatest diversity (2–13 spp) of fossils dominated by frondose *Fractofusus* and *Charnodiscus* was found in the Catalina pedotype (Hofmann et al., 2008), and comparable diversity (1–11 spp) is found in Maglona paleosols, such as surface E frequented by tourists (Clapham et al., 2003). Less diverse (1–6 spp) assemblages of fronds are found in very weakly developed Union and Acis pedotypes. Increased diversity has been attributed to ecological succession (Clapham et al., 2003), and this hypothesis is strongly supported here by increased thickness, bedding destruction, and chemical differentiation from Union–Acis to Catalina–Maglona pedotypes in concert with fossil diversity increase. The difference between gray pyritic (Murphy's) paleosols and red non-pyritic paleosols (Acis, Union, Maglona, and Catalina) in contrast follows an inferred ecological zonation along a hydrological gradient between waterlogged, chemically reducing and well-drained, chemically oxidizing soils (Retallack, 2014a). Pyritic Murphy's paleosols are identical to soils and paleosols of marine-influenced tidal flats, currently supporting salt marsh (Patching, 1987) or mangal (Altschuler et al., 1983; Retallack and Dilcher, 2012) vegetation. In contrast, red Acis, Union, Maglona, and Catalina pedotypes are comparable with soils of coastal floodplains, with a greater variety of plants (Cisternas et al., 2005; Patching, 1987).

The long geological record of intertidal salt marsh and mangal vegetation was always less diverse than freshwater coastal vegetation (Fig. 12). Intertidal woodlands include modern angiosperm mangrove genera back into the Tertiary (Retallack and Kirby, 2007) and extinct

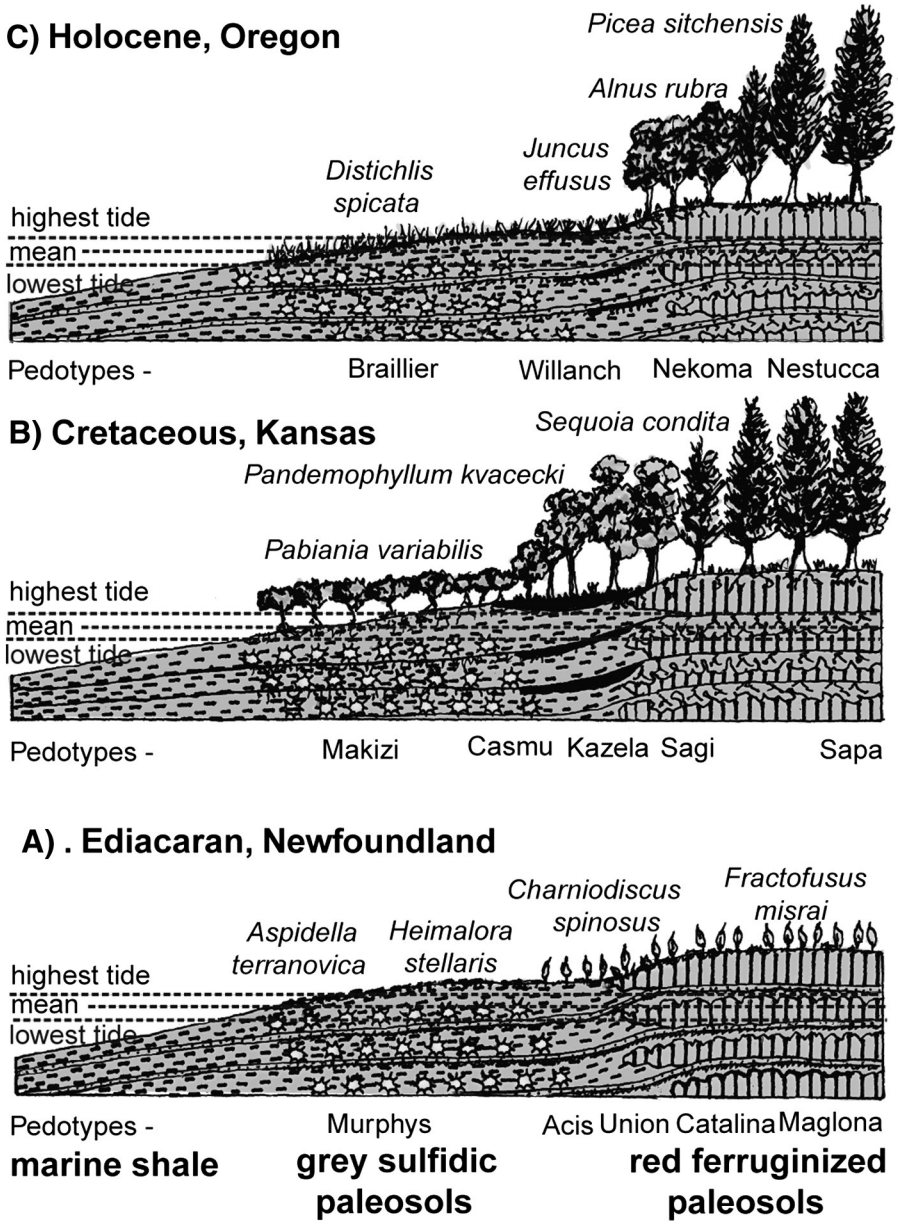

Fig. 12. Reconstructed ecological transect for the Ediacaran of Newfoundland (A), compared with vegetation in comparable Phanerozoic soils (B, C: after Patching, 1987; Retallack and Dilcher, 2012). The sulfidic grey intertidal pedofacies of the *Aspidella–Heimalora* community is comparable with soils of intertidal salt marsh and mangal. The mottled to red supratidal pedofacies of the *Charniodiscus–Fractofusus* community is comparable with soils of coastal woodlands and forests. Acis–Union paleosols supported early successional and Catalina–Maglona paleosols late successional communities.

angiosperm mangroves back to Cretaceous (Retallack and Dilcher, 2012). Other plants formed mangal in deep time, such as ferns in the Cretaceous (Smith et al., 2001), and early cladoxylaleans in the Devonian (Retallack and Huang, 2011). Enigmatic lichen-like nematophytes formed Silurian intertidal vegetation, when more diverse non-vascular plants occupied coastal plains (Retallack, 2015). Few plants are adapted to intertidal stresses, including osmotic stress of saltwater, searing by salt crystals, episodic storm surges, and stagnant groundwater, so that intertidal vegetation is low in diversity compared with that of well-drained coastal plains (Hacker and Gaines, 1997; Duke et al., 1998). Ediacaran organisms remain problematic but were lichen-like in form (Retallack, 2013b), attachment (Antcliffe et al., 2015), and reproduction (Mitchell et al., 2015), as well as showing low-diversity intertidal and diverse coastal plain communities (Fig. 13). Dramatic evolutionary differences in intertidal vegetation since the Ediacaran is reflected in the array of roots, rhizoids, and rhizines preserved in paleosols (Retallack, 2001), but the soil profiles themselves have changed little since that time. Ediacaran intertidal paleosols were gray, pyritic, and very weakly developed, and Ediacaran coastal plain paleosols red with green mottles and weakly to moderately developed, like modern profiles (Fig. 12). These differences extend to muted mineral and geochemical profiles in intertidal paleosols compared with coastal plain paleosols in Ediacaran (Fig. 5), as well as in geologically younger paleosols (Retallack and Huang, 2011; Retallack and Dilcher, 2012).

6. Conclusions

Sessile vendobionts of intertidal pyritic paleosols documented here refine the marine (Hofmann et al., 2008) versus terrestrial (Retallack, 2013b, 2014c) controversy concerning vendobionts, with an intermediate habitat comparable with that of salt marshes and mangroves (Fig. 12). Thus, some Ediacaran fossils have been found in intertidal facies, not only as drift specimens (Retallack, 2014d) but also in terrestrial red beds (Retallack, 2014c). Whole communities of Ediacaran fossils in

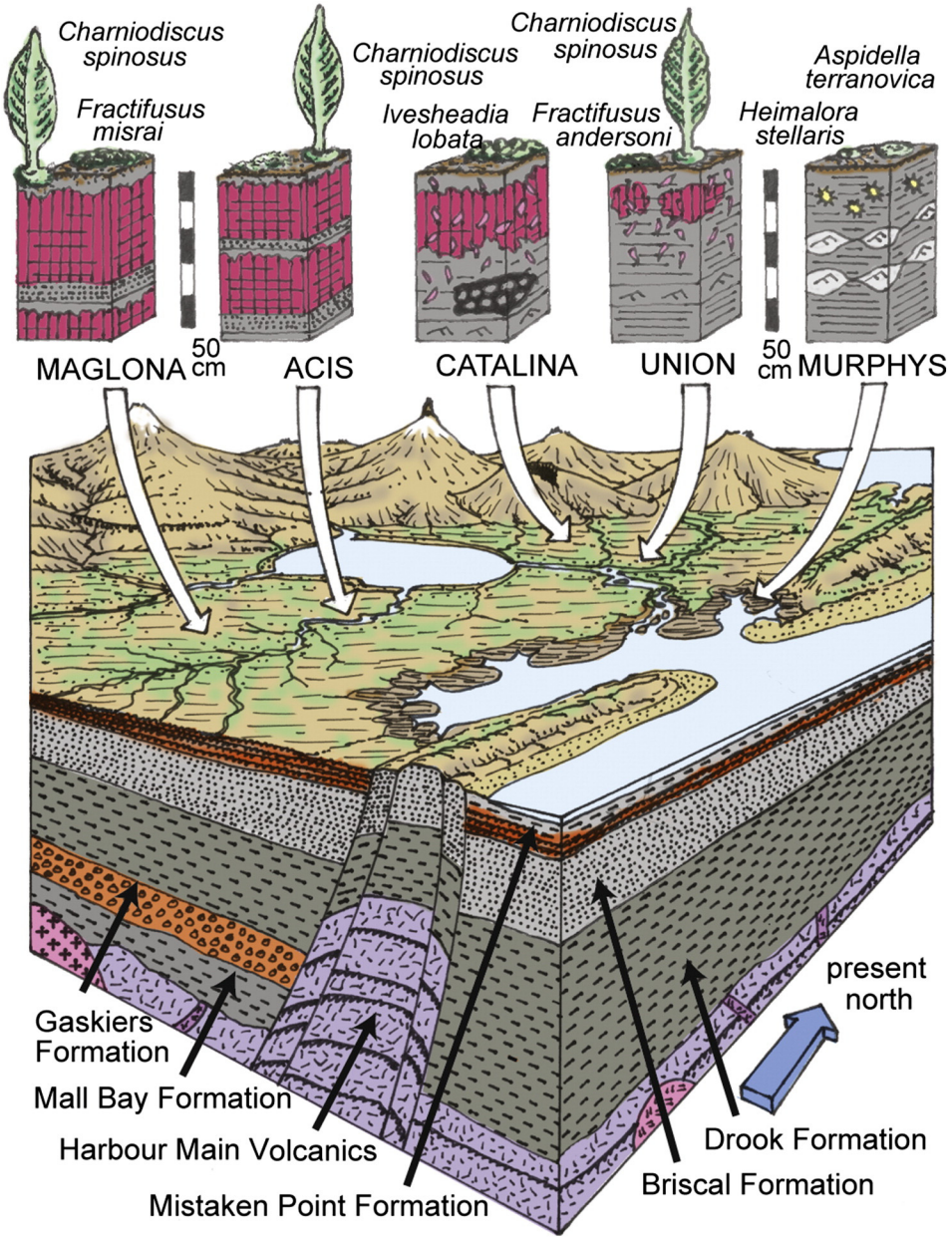

Fig. 13. Conjectural reconstruction of the sedimentary paleoenvironment of the Ediacaran (565 Ma) Mistaken Point Formation in Newfoundland (based on data from Retallack, 2014a).

life position on large slabs like those of the Mistaken Point and Drook Formations of Newfoundland are stunning tourist attractions that deserve World Heritage listing currently sought by Parks and Natural Areas Division of Newfoundland and Labrador. Interpreted as lichenized fungi (Retallack, 2014a), these Ediacaran communities were ecologically at least, as plant-like as they appear.

Fine grained intertidal to supratidal facies and paleosols as well as comparisons with Oregon (Heller et al., 1985; Ryu and Niem, 1999) and Chile (Atwater et al., 1992; Cisternas et al., 2005) support interpretation of the Trinity Bay Synclinorium as a forearc basin and of the Holyrood Horst as the central uplifted portion of a subduction complex (Fig. 13). The subduction zone would have been to the present east and the calcalkaline volcanic arc is still there to the west (Retallack, 2014a).

If Mistaken Point assemblages were organisms of intertidal to floodplain soils, it is unlikely that they were algae, sponges, cnidarians, or sea pens (Narbonne, 2005; Hofmann et al., 2008), which could not tolerate such exposure. Also unlikely was the locomotion of *Aspidella* (Menon et al., 2013) or other putative cnidarian trace fossils (Liu et al., 2010), which can be interpreted as growth rugae of sessile organisms (Retallack, 2014b) or as tilting trace tool marks (Retallack, 2010), respectively.

The variety of fossils in paleosols of the Mistaken Point Formation (Narbonne, 2005; Hofmann et al., 2008) may reflect a comparable variety of biological affinities (Liu et al., 2015). Fungal affinities for the large, foliose, quilted fossils (such as *Fractofusus* and *Charniodiscus*) have been argued by Peterson et al. (2003) from sessile habit, lack of mouth, anus, or body cavities, population structure of indeterminate growth, fractal-modular organization, mycelium-like structures, and strong resistance to burial compaction. For these same reasons, Ediacaran fossils of Newfoundland have long been regarded as osmotrophic (Clapham et al., 2003; Liu et al., 2015). Lichenization of Ediacaran fungi to include a photosynthetic symbiont (Retallack, 2013b) would explain foliose form, tiering, and limited-overlap of fossils on single paleosol surfaces (Clapham et al., 2003). Permineralized glomeromycotan lichens are known from the early Ediacaran (ca. 600 Ma) of China (Yuan et al., 2005), so that Mistaken Point fossils (465 Ma) would not have been the most ancient known lichens.

Acknowledgments

Fieldwork under permit from Parks and Natural Areas Division of Newfoundland and Labrador (director Siân French) was conducted with supervision and assistance of Richard Thomas. Nathalie Djan-Chekar curated polished slabs into collections of The Rooms (Provincial Museum), St. John's. Thanks are due to Guy Narbonne, Doug Erwin, Sarah Tweedt, Marc Laflamme, Paul Hoffman, and Nora Noffke for useful discussion.

References

Altschuler, Z.S., Schnepfe, M.M., Silber, C.C., Simon, F.O., 1983. Sulfur diagenesis in Everglades peat and the origin of pyrite in coal. Science 221, 221–227.
Anderson, M.M., Misra, S.B., 1968. Fossils found in the Pre-Cambrian Conception Group of south-eastern Newfoundland. Nature 220, 680–681.
Antcliffe, J.B., Hancy, A.D., Brasier, M.D., 2015. A new ecological model for the ~565 Ma Ediacaran biota of Mistaken Point, Newfoundland. Precambrian Research 268, 227–242.
Atwater, B.F., Hemphill-Haley, E., 1997. Recurrence intervals for great earthquakes of the past 3500 years at northeastern Willapa Bay, Washington: U.S. Geological Survey Professional Paper 1576, 1–108.
Atwater, B.F., Núñez, H.J., Vita-Finzi, C., 1992. New late Holocene emergence despite earthquake-induced submergence, south-central Chile. Quaternary International 15–16, 77–85.
Bamforth, E.L., Narbonne, G.M., 2009. New Ediacaran rangeomorphs from Mistaken Point, Newfoundland, Canada. Journal of Paleontology 83, 897–913.
Bamforth, E.L., Narbonne, G.M., Anderson, M.M., 2008. Growth and ecology of a multibranched Ediacaran rangeomorph from the Mistaken Point assemblage, Newfoundland. Journal of Paleontology 82, 763–777.
Benus, A.P., 1988. Sedimentological context of a deep-water Ediacaran fauna (Mistaken Point Formation, Avalon Zone, eastern Newfoundland). In: Landing, E., Narbonne, G.M., Myrow, P.M. (Eds.), Trace fossils, small shelly fossils, and the Precambrian–Cambrian Boundary. New York State Mus. Bull 463, pp. 8–9.
Berner, R.A., Raiswell, R., 1984. C/S method for distinguishing freshwater from marine rocks. Geology 12, 365–368.
Bouma, A.H., 1962. Sedimentology of some flysch deposits: a graphic approach to facies interpretation. Elsevier, Amsterdam.
Brasier, M.D., Antcliffe, J.B., 2009. Evolutionary relationships within the Avalonian Ediacara biota; new insights from laser analysis. Journal of the Geological Society of London 166, 363–384.
Brimhall, G.H., Chadwick, O.A., Lewis, C.J., Compston, W., Williams, I.S., Danti, K.J., Dietrich, W.E., Power, M.E., Hendricks, D., Bratt, J., 1992. Deformational mass transport and invasive processes in soil evolution. Science 255, 695–702.
Canfield, D.E., Poulton, S.W., Narbonne, G.M., 2007. Late Neoproterozoic deep-ocean oxygenation and the rise of animal life. Science 315, 92–95.
Canfield, D.E., Farquhar, J., Zerkle, A.L., 2010. High isotope fractionations during sulfate reduction in a low-sulfate euxinic ocean analog. Geology 38, 415–418.
Cisternas, M., Atwater, B.F., Torrejón, F., Sawai, Y., Machuca, G., Lagos, M., Eipert, A., Youlton, C., Salgado, I., Kamataki, T., Shishikura, M., Rajendran, C.P., Malik, J.K., Rizal, Y., Husni, M., 2005. Predecessors of the giant 1960 Chile earthquake. Nature 437, 404–407.
Clapham, M.E., Narbonne, G.M., Gehling, J.G., 2003. Paleoecology of the oldest known animal communities; Ediacaran assemblages at Mistaken Point, Newfoundland. Paleobiology 29, 527–544.
Clapham, M.E., Narbonne, G.M., Gehling, J.G., Greentree, C., Anderson, M.M., 2004. *Thectardis avalonensis*; a new Ediacaran fossil from the Mistaken Point biota, Newfoundland. Journal of Paleontology 78, 1031–1036.
Cuthill, J.F.H., Conway Morris, S., 2014. Fractal branching of Ediacaran rangeomorph fronds reveal a lost Proterozoic body plan. Proceedings of the National Academy of Sciences 111, 13122–13126.
Dalrymple, R.W., Gehling, J.G., Narbonne, G., 1999. Storm-dominated sedimentation in a tectonically active basin; implications for the paleoecology of the Ediacaran (Neoproterozoic) biota at Mistaken Point, Newfoundland. Abstracts of the Geological Society of America 31 (7), 362.
Darroch, S.A.F., Laflamme, M., Clapham, M.E., 2013. Population structure of the oldest known macroscopic communities from Mistaken Point, Newfoundland. Paleobiology 39, 591–608.
Dashtgard, S.E., Gingras, M.K., MacEachern, J.A., 2009. Tidally modulated shorefaces. Journal of Sedimentary Research 79, 793–807.
DiMichele, W.A., Falcon-Lang, H.J., 2011. Pennsylvanian 'fossil forests' in growth position (T0 assemblages): origin, taphonomic bias and palaeoecological insights. Journal of the Geological Society of London 168, 585–605.
Dott, R.H., Bourgeois, J., 1982. Hummocky stratification: significance of its variable bedding sequences. Bulletin of the Geological Society of America 93, 663–680.
Dover, J.H., Berry, W.B.N., Ross, R.J., 1980. Ordovician and Silurian Phi Kappa and Trail Creek Formation, Pioneer Mountains, Central Idaho—Stratigraphic and Structural Revisions, and New Data on Graptolite Faunas. Profession Paper of the U.S. Geological Survey 1090, 1–54.
Duke, N.C., Ball, M.C., Ellison, J.C., 1998. Factors influencing biodiversity and distributional gradients in mangroves. Global Ecology and Biogeography Letters 7, 27–47.
Evans, D.A.D., Raub, T.D., 2011. Neoproterozoic palaeolatitudes: a global update. In: Arnaud, E., Halverson, G.P., Shields-Zhou, G. (Eds.), The geological record of Neoproterozoic glaciations. Memoir of the Geological Society of London 36, pp. 93–112.
Fischer, A.G., 1965. Fossils, early life, and atmospheric history. Proceedings of the National Academy of Sciences 53, 1205–1215.
Flude, L.I., Narbonne, G.M., 2008. Taphonomy and ontogeny of a multibranched Ediacaran fossil; *Bradgatia* from the Avalon Peninsula of Newfoundland. Canadian Journal of Earth Sciences 45, 1095–1109.
Food and Agriculture Organization, 1971. Soil Map of the World, vol.IV, South America. United Nations Educational and Cultural Organization, Paris.
Food and Agriculture Organization, 1974. Soil Map of the World, vol. 1, Legend. United Nations Educational and Cultural Organization, Paris.
Gehling, J.G., 1999. Microbial mats in terminal Proterozoic siliciclastics: Ediacaran death masks. Palaios 14, 40–57.
Gehling, J.G., Narbonne, G.M., 2007. Spindle-shaped Ediacara fossils from the Mistaken Point assemblage, Avalon Zone, Newfoundland. Canadian Journal of Earth Sciences 44, 367–387.
Hacker, S.D., Gaines, S.D., 1997. Some implications of direct positive interactions for community species diversity. Ecology 78, 1990–2003.
Hebert, C.L., Kaufman, A.J., Penniston-Dorland, S.C., Martin, A.J., 2010. Radiometric and stratigraphic constraints on terminal Edicaran (post-Gaskiers) glaciation and metazoan evolution. Precambrian Research 182, 402–414.
Heller, P.L., Peterman, Z.E., O'Neil, J.R., Shafiqullah, M., 1985. Isotopic provenance of sandstones from the Eocene Tyee Formation, Oregon Coast Range. Bulletin of the Geological Society of America 96, 770–780.
Higgs, R., 2011. 'Hummocky cross-stratification-like structures in deep-sea turbidites: Upper Cretaceous Basque basins (Western Pyrenees, France)' by Mulder et al. (2009): discussion. Sedimentology 58, 566–570.
Hofmann, H.J., O'Brien, S.J., King, A.F., 2008. Ediacaran biota on Bonavista Peninsula, Newfoundland, Canada. Journal of Paleontology 82, 1–36.
Isbell, R.F., 1996. The Australian Soil Classification. C.S.I.R.O. Press, Melbourne.
Ito, M., Katsura, Y., 1992. Inferred glacio-eustatic control for high-frequency depositional sequences of the Plio-Pleistocene Kazusa Group, a forearc basin fill in Boso Peninsula, Japan. Sedimentary Geology 80, 67–75.
Jagodzinski, E.A., Black, L.P., 1999. U–Pb dating of silicic lavas, sills and syneruptive resedimented volcaniclastic deposits of the Lower Devonian Crudine Group, Hill End Trough, New South Wales. Australian Journal of Earth Sciences 46, 749–764.

Jashemski, W.F., 1979. The Gardens of Pompeii, Herculaneum and the Villas Destroyed by Vesuvius. Caratzas Bros, New Rochelle.
King, A.F., 1988. Geology of the Avalon Peninsula, Newfoundland. Newfoundland Department of Mines Map. 88 p. 01.
Ku, T.C.W., Kay, J., Browne, E., Martini, A.M., Peters, S.C., Chen, M.D., 2008. Pyritization of iron in tropical coastal sediments: implications for the development of iron, sulfur, and carbon diagenetic properties, Saint Lucia, Lesser Antilles. Marine Geology 249, 184–205.
Laflamme, M., Narbonne, G.M., Anderson, M.M., 2004. Morphometric analysis of the Ediacaran frond *Charniodiscus* from the Mistaken Point Formation, Newfoundland. Journal of Paleontology 78, 827–837.
Liu, A.G., McIlroy, D., Brasier, M.D., 2010. First evidence for locomotion in the Ediacara biota from the 565 Ma Mistaken Point Formation, Newfoundland. Geology 38, 123–126.
Liu, A.G., Kenchington, C.G., Mitchell, E.G., 2015. Remarkable insights into the paleoecology of the Avalonian Ediacaran macrobiota. Gondwana Research 27, 1355–1380.
Ludlam, S.D., 1974. Fayetteville Green Lake, New York. 6. The role of turbidity currents in lake sedimentation. Limnology and Oceanography 19, 656–664.
McClaughry, J.D., Wiley, T.J., Ferns, M.L., Madin, I.P., 2010. Digital Geologic Map of the Southern Willamette Valley, Benton, Lane, Linn, Marion and Polk Counties, Oregon. Oregon Department of Geology and Mineral Industries Open File Rept O-10-03pp. 1–116.
McMenamin, M.A.S., 1986. The garden of Ediacara. Palaios 1, 178–182.
Menon, L.R., McIlroy, D., Brasier, M.D., 2013. Evidence for Cnidaria-like behavior in ca. 560 Ma Ediacaran *Aspidella*. Geology 41, 895–897.
Misra, S.B., 1971. Stratigraphy and depositional history of late Precambrian coelenterate-bearing rocks, southeastern Newfoundland. Bulletin of the Geological Society of America 82, 979–987.
Mitchell, E.G., Kenchington, C.G., Liu, A.G., Matthews, J.J., Butterfield, N.J., 2015. Reconstructing the reproductive mode of an Ediacaran macro-organism. Nature 524, 343–346.
Murphy, C.P., 1983. Point counting pores and illuvial clay in thin section. Geoderma 31, 133–150.
Narbonne, G.M., 2005. The Ediacara biota: Neoproterozoic origin of animals and their ecosystems. Annual Review of Earth and Planetary Sciences 33, 421–442.
Narbonne, G.M., Dalrymple, R.W., Laflamme, M., Gehling, J.G., Boyce, W.D., 2005. Life after snowball; the Mistaken Point biota and the Cambrian of Avalon: North American Paleontological Convention Excursion Guide, 1–33.
Narbonne, G.M., Laflamme, M., Greentree, C., Trusler, P., 2009. Reconstructing a lost world; Ediacaran rangeomorphs from Spaniard's Bay, Newfoundland. Journal of Paleontology 83, 503–523.
Neaman, A., Chorover, J., Brantley, S.L., 2005. Implications of the evolution of organic acid moieties for basalt weathering over geological time. American Journal of Science 305, 147–185.
Noble, S.R., Condon, D.J., Carney, J.N., Wilby, P.R., Pharaoh, T.C., Ford, T.D., 2015. U–Pb geochronology and global context of the Charnian Supergroup, UK: constraints on the age of key Ediacaran fossil assemblages. Bulletin of the Geological Society of America 127, 250–265.
O'Brien, S.J., King, A.F., 2004. Late Neoproterozoic to early Paleozoic stratigraphy of the Avalon Zone in the Bonavista Peninsula, Newfoundland: an update. Geological Survey of Newfoundland Current Research 04–1, 213–224.
Óskarsson, B.V., Riishuus, M.S., Arnalds, O., 2012. Climate-dependent chemical weathering of volcanic soils in Iceland. Geoderma 189–190, 635–651.
Papezik, V.S., 1974. Prehnite-pumpellyite facies metamorphism of late Precambrian rocks of the Avalon Peninsula. Canadian Mineralogist 12, 463–468.
Parsons, R.C., 2011. Cape Race: stories from the coast that sank the Titanic. Flanker Press, St Johns.
Patching, W.R., 1987. Soil Survey of Lane County Area, Oregon. U.S. Soil Conservation Service, Washington DC.
Percival, I.G., Glen, R.A., 2007. Ordovician to earliest Silurian history of the Macquarie Arc, Lachlan Orogen, New South Wales. Australian Journal of Earth Sciences 54, 143–165.
Peters, R., Jaffe, B., Gelfenbaum, G., 2007. Distribution and sedimentary characteristics of tsunami deposits along Cascadia margin of North America. Sedimentary Geology 200, 372–386.
Peterson, K.J., Waggoner, B., Hagadorn, J.W., 2003. A fungal analog for Newfoundland Ediacaran fossils? Integrative and Comparative Biology 43, 127–136.
Pisarevsky, S.A., McCausland, P.J.A., Hodych, J.P., O'Brien, S.J., Tait, J.A., Murphy, J.B., 2012. Paleomagnetic study of the late Neoproterozic Bull Arm and Crown Hill Formations (Musgravetown Group) of eastern Newfoundland: implications for Avalonia and West Gondwana paleogeography. Canadian Journal of Earth Sciences 49, 308–327.
Raiswell, R., Berner, R.A., 1986. Pyrite and organic matter in Phanerozoic normal marine shales. Geochimica et Cosmochimica Acta 50, 1967–1976.
Retallack, G.J., 1997. A Colour Guide to Paleosols. Wiley, Chichester.
Retallack, G.J., 2001. Soils of the Past. Blackwell, Oxford.
Retallack, G.J., 2008. Cambrian palaeosols and landscapes of South Australia. Australian Journal of Earth Sciences 55, 1083–1106.
Retallack, G.J., 2010. First evidence for locomotion in the Ediacara biota from the 565 Ma Mistaken Point Formation, Newfoundland: comment. Geology 38, e223.
Retallack, G.J., 2011. Exceptional fossil preservation during CO_2 greenhouse crises? Palaeogeography Palaeoclimatology Palaeoecology 307, 59–74.
Retallack, G.J., 2013a. Ediacaran Gaskiers Glaciation of Newfoundland reconsidered. Journal of the Geological Society of London 170, 19–36.
Retallack, G.J., 2013b. Ediacaran life on land. Nature 493, 89–92.
Retallack, G.J., 2013c. Early Cambrian humid, tropical paleosols from Montana. In: Driese, S.G. (Ed.), New frontiers in paleopedology and terrestrial paleoclimatology. Society of Economic Paleontologists and Mineralogists Special Paper 44, pp. 257–272.
Retallack, G.J., 2014a. Volcanosedimentary paleoenvironments of Ediacaran fossils in Newfoundland. Bulletin of the Geological Society of America 126, 619–638.
Retallack, G.J., 2014b. In: Menon, L.R., McIlroy, D., Brasier, M.D. (Eds.), Comment on "Evidence for Cnidaria-like behavior in c. 560 Ma Ediacaran *Aspidella*". Geology 42, p. e323.
Retallack, G.J., 2014c. Precambrian life on land. Palaeobotanist 63, 1–15.
Retallack, G.J., 2014d. In: Xiao, S., Droser, M., Gehling, J.G., Hughes, I.V., Wan, B., Chen, Z., Yuan, X. (Eds.), Comment on "Affirming life aquatic for the Ediacara biota in China and Australia". Geology 42, p. e325.
Retallack, G.J., 2015. Reassessment of the Silurian problematicum Rutgersella as another post-Ediacaran vendobiont. Alcheringa 39, 573–588.
Retallack, G.J., Dilcher, D.L., 2012. Core and geophysical logs versus outcrop for interpretation of Cretaceous paleosols in the Dakota Formation of Kansas. Palaeogeography Palaeoclimatology Palaeoecology 329–330, 47–63.
Retallack, G.J., Huang, C.-M., 2011. Ecology and evolution of Devonian trees in New York, USA. Palaeogeography Palaeoclimatology Palaeoecology 299, 110–128.
Retallack, G.J., Kirby, M.X., 2007. Middle Miocene global change and paleogeography of Panama. Palaios 22, 667–679.
Retallack, G.J., Marconato, A., Osterhout, J.T., Watts, K.E., Bindeman, I., 2014. Revised Wonoka isotopic anomaly in South Australia and Late Ediacaran mass extinction. Journal of the Geological Society of London 171, 709–722.
Ryu, I.-C., 2007. Source rock characterization and petroleum systems of Eocene Tyee basin, southern Oregon Coast Range, USA. Organic Geochemistry 39, 75–90.
Ryu, I.-C., Niem, A.R., 1999. Sandstone diagenesis, reservoir potential, and sequence stratigraphy of the Eocene Tyee Basin, Oregon. Journal of Sedimentary Research 69, 384–393.
Seilacher, A., 1982. Distinctive features of sandy tempestites. In: Einsele, G., Seilacher, A. (Eds.), Cyclic and Event Stratification. Springer, Berlin, pp. 333–349.
Seilacher, A., 1984. Late Precambrian and Early Cambrian Metazoa: preservational or real exinctions? In: Holland, H.D., Trendall, A.F. (Eds.), Patterns of Change in Earth Evolution. Springer, Berlin, pp. 159–168
Seilacher, A., 1989. Vendozoa: organismic construction in the Proterozoic biosphere. Lethaia 22, 229–239.
Sheldon, N.D., Retallack, G.J., Tanaka, S., 2002. Geochemical climofunctions from North American soils and application to paleosols across the Eocene–Oligocene boundary in Oregon. Journal of Geology 110, 687–696.
Smith, J.B., Lamanna, M.C., Lacovara, K.J., Dodson, P., Smith, J.R., Poole, J.C., Giegengack, R., Attia, Y., 2001. A giant sauropod dinosaur from an Upper Cretaceous mangrove deposit in Egypt. Science 291, 1704–1706.
Snavely, P.D., Wagner, H.C., MacLeod, N.S., 1964. Rhythmic-bedded eugeosynclinal deposits of the Tyee Formation, Oregon Coast Range. In: Merriam, D.F. (Ed.), Symposium on cyclic sedimentation. Bulletin of the Kansas Geological Survey 169, pp. 461–480.
Soil Survey Staff, 2010. Keys to Soil Taxonomy. USDA-Natural Resources Conservation Service, Washington DC.
Stevens, N.C., 1957. Further notes on the Ordovician Formations of central New South Wales. Journal and Proceedings. Royal Society of New South Wales 90, 44–50.
Sutcliffe, O.E., Briggs, D.E.G., Bartels, C., 1999. Ichnological evidence for the environmental setting of the Fossil-Lagerstätten in the Devonian Hunsrück Slate, Germany. Geology 27, 275–278.
Szczuciński, W., Kokociński, M., Rzeszewski, M., Chagué-Goff, C., Cachão, M., Goto, K., Sugawara, D., 2012. Sediment sources and sedimentation processes of 2011 Tohoku-oki tsunami deposits on Sendai Plain, Japan—insights from diatoms, nannoliths and grain size distribution. Sedimentary Geology 282, 40–56.
Takashima, R., Kawabe, F., Nishi, H., Moriya, K., Wanid, R., Ando, H., 2004. Geology and stratigraphy of forearc basin sediments in Hokkaido, Japan: Cretaceous environmental events on the north-west Pacific margin. Cretaceous Research 25, 365–390.
Talling, P.J., Masson, D.G., Sumner, E.J., Malgesini, G., 2012. Subaqueous density flows: depositional processes and deposit types. Sedimentology 59, 1937–2003.
Tarhan, L.G., Droser, M.L., Gehling, J.G., Tsaugis, M.P., 2015. Taphonomy and morphology of the Ediacara form genus *Aspidella*. Precambrian Research 257, 124–136.
Thompson, M.D., Barr, S.M., Grunow, A.M., 2012. Avalonian perspectives on neoproterozoic paleogeography: evidence from Sm-Nd isotope geochemistry and detrital zircon geochronology in SE New England, USA. Bulletin of the Geological Society of America 124, 517–531.
Van Kranendonk, M.J., Gehling, J.G., Shields, G.A., 2008. Precambrian. In: Ogg, J.G., Ogg, G., Gradstein, F.M. (Eds.), The Concise Geologic Time Scale. Cambridge University Press, Cambridge, UK, pp. 23–36.
Van Sickel, W.A., Kominz, M.A., Miller, K.G., Browning, J.V., 2004. Late Cretaceousand Cenozoic sea-level estimates: backstripping analysis of borehole data, onshore New Jersey. Basin Research 16, 451–465.
Veblen, T.T., Ashton, D.H., 1978. Catastrophic influences on vegetation of the Valdivian Andes, Chile: Vegetatio. 36 pp. 149–167.
Weatherby, D.G., 1991, Stratigraphy and sedimentology of the late Eocene Bateman Formation, southern Oregon Coast Range. Unpublished MSc thesis, Department of Geological Sciences, University of Oregon.
Yuan, X., Xiao, S., Taylor, T.N., 2005. Lichen-like symbiosis 600 million years ago. Science 308, 1017–1020.
Zachos, J., Pagani, M., Sloan, L., Ellen Thomas, E., Billups, K., 2001. Trends, rhythms, and aberrations in global climate 65 Ma to present. Science 292, 292–686.